Heliyon 10 (2024) e32625

Contents lists available at ScienceDirect

Heliyon

journal homepage: www.cell.com/heliyon

Research article

Influence of climate variability and land cover dynamics on the spatio-temporal NDVI patterns in western hydrological regions of Bangladesh

Jumana Akhter [a,*], Rounak Afroz [b]

[a] Department of Civil Engineering, Military Institute of Science and Technology, Mirpur Cantonment, Dhaka, 1216, Bangladesh
[b] Department of Water Resources Engineering, Bangladesh University of Engineering and Technology, Dhaka, 1000, Bangladesh

ARTICLE INFO

Keywords:
Normalized difference vegetation index
Climatic variables
Land cover changes
Bangladesh

ABSTRACT

Analyzing vegetation greenness considering climate and land cover changes is crucial for Bangladesh given the historically drier North-West and South-West regions of Bangladesh have shown prominent climatic and hydrological variations. Therefore, this study assessed the spatial and temporal variation of NDVI and its relationship with climate and land cover changes from 2000 to 2022 for these regions. In this study, Moran's I and Getis Ord Gi* were employed for spatial autocorrelation and Mann-Kendall, Sen's slope test along with Innovative Trend Analysis were deployed to identify temporal trends of NDVI. RMSE, MAE and R-squared values were assessed between computed and observed PET. Correlation of NDVI with climate variables were assessed through multivariate correlation analysis and correlation mapping. Additionally, Pearson product moment correlation was applied between different types of land cover and NDVI. Spatial autocorrelation outcomes showed that NDVI values have been clustered in distinct hot-spots and cold-spots over the years. Temporal trend detection results indicate that NDVI values are rising significantly all over the regions. Multivariate correlation analysis identified no climate variable to be the limiting factor for NDVI changes. Similarly, the precipitation-NDVI correlation map displayed no significant correlation. Nonetheless, temperature-NDVI correlation map illustrated varying degrees of mostly moderate and strong positive correlations with distinct negative correlation results in the Sundarbans of South-West region. Land cover pattern analysis with NDVI showed a positive correlation to forest, cropland and vegetation area increasing and negative correlation to grassland and barren area decreasing. In this regard, Rangpur division exhibited stronger correlations than Rajshahi division in North-West. The findings indicate that NDVI changes in the regions are largely dependent on land cover changes in comparison to climate trends. This can instigate further research in other hydrological regions to explore the natural and man-made factors that can affect the greenery and vegetation density in specific regions.

1. Introduction

In the face of continuous anthropogenic activities and their far-reaching consequences, climate change has accelerated and remained one of the most formidable global challenges. It has disastrous consequences on environment, vegetation dynamics, agri-

* Corresponding author.
E-mail addresses: tanuja.jt41@gmail.com (J. Akhter), rounak@wre.buet.ac.bd (R. Afroz).

https://doi.org/10.1016/j.heliyon.2024.e32625
Received 31 January 2024; Received in revised form 5 June 2024; Accepted 6 June 2024
Available online 8 June 2024

culture and subsequent food security; especially in the developing countries. Bangladesh is one of the most climate-vulnerable countries in the world as the agriculture and food production are impacted and constrained by seasonal variability, and climatic variables in this country [1]. Although climate change had adverse impacts all around Bangladesh, the northwestern districts and some of the southwestern districts are the worst-sufferer compared to other hydrological regions of the country [2,3]. North-West (NW) region is characterized by semi-arid climate and below average rainfall ranging from 1400 mm to 2200 mm [4,5]. On the other hand, South-West (SW) region is slightly more humid due to its proximity to the Bay of Bengals but with an average rainfall below 1400 mm [6]. The temperature of the regions varies between $25^{\circ}C\ to\ 35^{\circ}C$ for maximum temperature and $10^{\circ}C\ to\ 20^{\circ}C$ for minimum temperature [7]. Other climatic variables such as PET, sunshine hours vary seasonally and spatially with different levels of drought risk in the regions [8–12]. Hence, the need to understand the spatio-temporal relationship between climate change variables, human activities and vegetation dynamics in the North-West (NW) and South-West (SW) regions of Bangladesh is significant for local adaptation and mitigation plans [13].

Vegetation is one of the most important links to regulate climate establishing interrelations among climate, hydrology, soil moisture and human activities [14,15]. Climate factors and variables along with anthropogenic activities affect the spatial and temporal dynamics of vegetation cover [16,17] Remote sensing methodologies using comprehensive spatial and temporal datasets have been widely employed in studies focusing on vegetation monitoring to identify trends and patterns responses to climate variability [18–23]. There have been various Standardized Vegetation indices (SVI) in use for assessing vegetation health such as NDVI, VCI, EVI etc. Normalized Difference Vegetation Index (NDVI) has been regarded a widely used and effective tool among them as it provides a comprehensive measurement of vegetation greenness and photosynthesis activity by capturing spectral reflectance of vegetation through remote sensing [24–29]. Vegetation greenness depends on several indicators such as temperature, precipitation, solar radiation, increase in average leaf size and area, number of leaves per plant, plant density, species, leaf growing season, areas of crops grown and numbers of crops grown [17,30]. Increment of NDVI values indicate an increase in more greenery in terms of area and intensity and degradation of the greenery and ecosystem would get reflected with a decrement in NDVI values [31–36]. Time series analysis of NDVI values provide accurate and efficient results when detecting changes in vegetation cover, mapping forest disturbance and classifying land use and land cover [37–39]. This has led to numerous studies in the past decade covering different parts of the world using different NDVI datasets such as MODIS, Landsat, NOAA-AVHRR with various statistical to assess the existence and extent of correlation of climatic and meteorological variables [40–43]. As the MODIS data products have been temporally consistent since 2000s and better for assessing vegetation changes in arid and semi-arid areas, recent studies have been increasingly using MODIS datasets [44,45]. Various studies demonstrated that the magnitude and timing of peak NDVI showed significant variability across different study sites across the sites based on seasonality with relatively high values of statistical parameters [46–49]. Spatial and temporal changes in vegetation health based on NDVI and its relationship with climate change variables and human activities were studied predominantly for Asian and African regions too. These studies used linear trend analysis, correlation analysis, ordinary least squares and buffer analysis to examine the most important indicators for different provinces or river basins [16,50–54]. Similarly, for studies covering South-Asia, results predicted vegetation and land use changes to be severely important to efficiently adapt to climate change impacts by analyzing NDVI time series for historical base periods and future predictions [55–59]. For Bangladesh, vegetation response to the effect of climate change was mostly studied for NW region [60–62] where fluctuations in vegetation density and intensity have been extensively evaluated by NDVI in conjecture with climate variables [63–66]. Moreover, being a primary parameter in various climate change studies, land use have shown to impact regional and global climate because of the influence anthropogenic activities [10,67–71]. Hence, there have been many studies based on land use changes for different study areas using advanced remote sensing datasets and approaches where both responses to climate because of land use and land cover changes, and changing land use patterns because of changing climate have been assessed [72–75]. In Bangladesh where anthropogenic changes like population and economy growth, infrastructure building along with biophysical factors, hydroclimatic variations and climate change are prominent, land use patterns are assessed based on NDVI studies in the recent decade [76–78]. While previous studies in Bangladesh have extensively analyzed these factors individually, concurrent assessment of combined influence of climatic variables and land cover changes on vegetation dynamics in critical hydrogeological zones remains scarce in current literature. Hence, understanding how changes in climate variables and land use patterns interact with vegetation greenness using NDVI datasets and integrating observed and remote sensing data with advanced analytical techniques are crucial in understanding the effects of climate change in NW and SW region of Bangladesh.

Several spatial autocorrelation studies of NDVI values quantify to which degree neighboring geographical units exhibit similar and different values or range to find out the spatial patterns of vegetation dynamics [52,79–82]. Quantitative analytical studies for detecting temporal trend are mostly based on non-parametric tests as they are better suited to deal with non-normally distributed hydrometeorology data than parametric methods [83]. The Mann-Kendall test and Sen's slope have been the most widely used nonparametric trend detection tests in many hydrological and vegetation index based studies [84–87]. Though bigger sample sizes throughout multiple decades make the tests more powerful, Mann Kendall has some restrictive assumptions such as data are serially independent, normality of the distribution and the length of the data along with assessing only the existence of monotonic trend [88]. Unlike Mann Kendall and Sen's slope test, Innovative Trend Analysis (ITA) is free from such assumptions and can detect both monotonic and non-monotonic trends [89]. Hence, increasingly ITA has been adopted in recent hydrological and environmental studies to detect changes and patterns [90–92]. Multivariate correlation analysis has proven to be an effective and multidimensional time series analysis in contemporary studies to assess the relationship among various interconnected meteorological and hydrological variables, vegetation indices and land use/cover parameters [93–95]. Additionally, Pearson correlation coefficient has been a widely used statistical method in studies between land use changes and its impact on vegetation cover and climatic variables in many climate critical areas [96–98].

In this study, 16-day 250 m MODIS NDVI, observed and gridded climatic variables-precipitation, maximum and minimum temperature, potential evapotranspiration and yearly 500 m MODIS Land cover datasets were analyzed to estimate trends, correlation and similarity in the North-West (NW) and South-West (SW) regions of Bangladesh. The notable contributions of this work are-

- Assessing and illustrating the spatial and temporal variation of NDVI in dry season for NW and SW regions from 2000 to 2022.

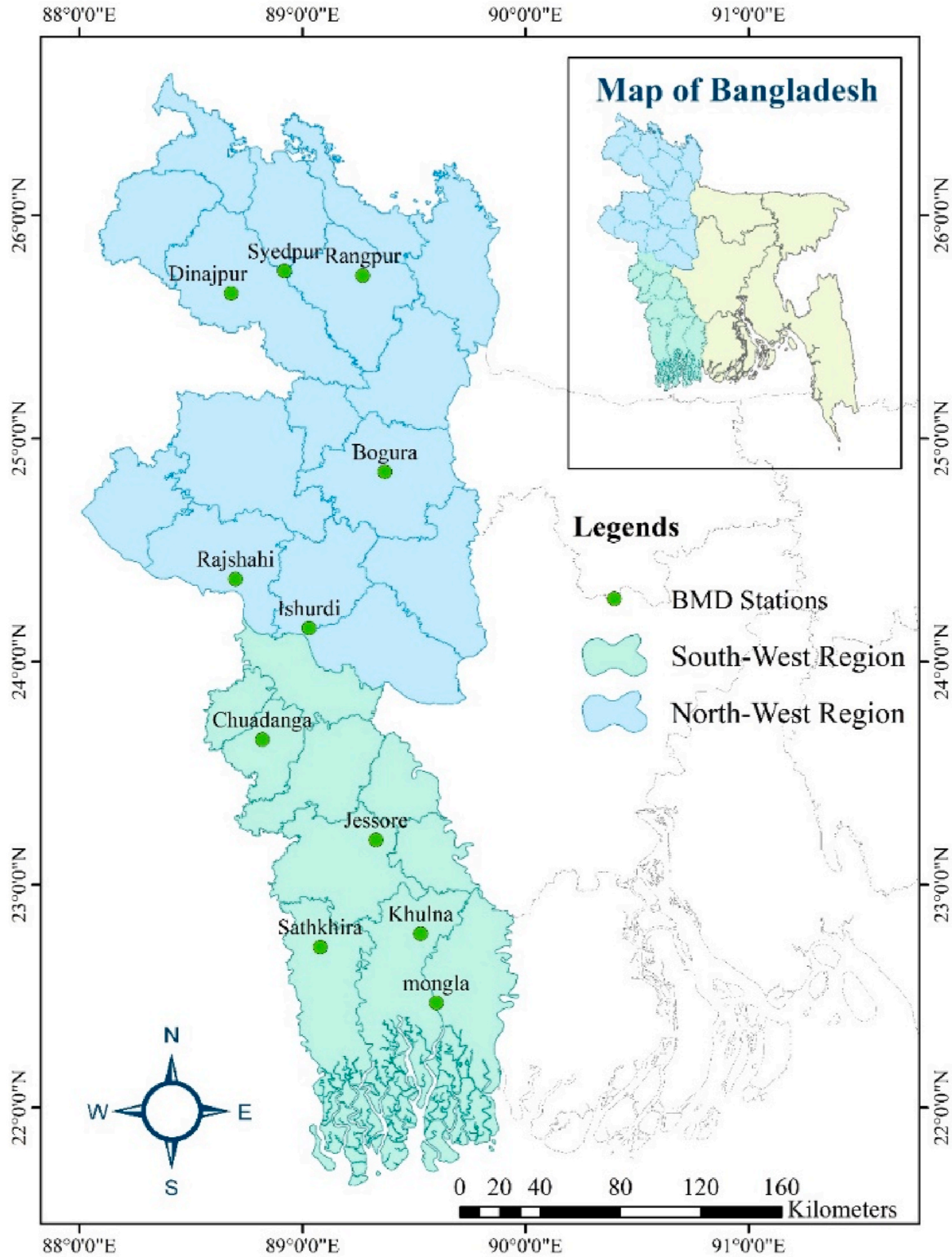

Fig. 1. Study Area (North-West and South-West hydrological region of Bangladesh). The 11 BMD stations situated in the regions are denoted in the figure.

- Establishing the spatial and temporal correlation between NDVI changes and climate variables (both observed and remote sensed) in NW and SW regions since 2000 to 2022.
- Exhibiting the trends of annual land cover changes of the regions from 2001 to 2022 and evaluating the correlation of NDVI changes with land cover change patterns.
- Demonstrating and discussing the interconnectedness of NDVI, climate and land cover changes in the historically hydro-critical NW and SW regions of Bangladesh.

The findings of this research can hold significant implications for both policy making and further studies by elucidating the extent of effects of both climate variables and land cover changes on greenery and vegetation dynamics in drier hydrologically critical areas of Bangladesh. Policymakers can assess which variables to focus on more and develop targeted strategies for climate adaptation and sustainable land management using the quantitative results of the study. Moreover, this work can provide a foundation for future research into the complex interactions of climate-land-vegetation and shaping ecosystems and frameworks tailored to different regions in Bangladesh and beyond.

2. Materials and methods

2.1. Study area

The study area for this study, shown in Fig. 1, consists of the North-West (NW) and South-West (SW) regions, two of eight hydrological regions of Bangladesh. They have 3 divisions- Rajshahi, Rangpur and Khulna and 26 administrative districts- Dinajpur, Kurigram, Gaibanda, Lalmonirhat, Nilphamari, Panchgarh, Rangour, Thakurgaon, Rajshahi, Nawabganj, Natore, Pabna, Sirajganj, Bogra, Jaipurhat, Naogaon, Bagerhat, Chuadanga, Jessore, Jhenaidah, Khulna, Kushtia, Magura, Meherpur, Narail and Sathkhira in the region. NW region lies in between 24°30′N and 26° 40′N latitudes and between 88° 01′E and 89° 90′E longitudes. And the SW lies between 21°35′N and 24°11′N latitudes and between 88°33′E to 89°57′E. There are 11 meteorological stations operated by Bangladesh Meteorological Department (BMD) in the regions. The locations of these BMD stations are denoted in Fig. 1, the study area map.

2.2. Data collection and processing

In this study, three types of data- Vegetation Index (NDVI) data, climatic data (Precipitation, temperature and potential-evapotranspiration data) and Land use data from 2000 to 2022, were utilized as shown in Table 1. The table shows the details of the spatial and temporal resolution of the data used along with the product name, dataset provider and the years they were extracted for.

2.3. NDVI

NDVI (Normalized Difference Vegetation Index) is a function of two bands and detects and quantifies the presence of live green vegetation using this reflected light in the visible and near-infrared bands (Garrigues et al., 2007).

NDVI = (Infrared – Red)/(Infrared + Red) (Li et al., 2014).

In this study, NDVI values were extracted for distinct points with various resolution as shapefiles, shown in Fig. 2. Fig. 2(a) shows NDVI extraction points based on each union of the study area for utilizing the values in spatial autocorrelation analysis whereas Fig. 2 (b) and (c) show the extraction points for utilizing the values in correlation mapping.

2.4. Methodology

Five types of analysis were done in this study as shown in Fig. 3 For spatial correlation, two methods- Moran's I Statistics and Getis Ord Gi* and for temporal analysis, Man-Kendall, Sen's slope test and Innovative Trend Analysis were conducted. PET was calculated using Hargreaves Samani equation because of the lack of availability of observed continuous PET values. Calculated PET was put against observed PET to test its efficacy by finding out the RMSE, MAE and R-squared values for each BMD stations. Then, for multivariate analysis, correlation was done with NDVI and Climatic variables for BMD stations. Gridded climate precipitation and

Table 1
Data Types and Sources with their properties.

Data	Product Name	Dataset Provider	Spatial Resolution	Temporal Resolution	Date
NDVI	MOD13Q1 V6.1	NASA LP DAAC	250 m	16-day	2000–2022
Precipitation	Total Precipitation	BMD	BMD stations	Monthly	2000–2022
	Total Precipitation	CHIRPS	0.05 ° X0.05 °	Monthly	2000–2022
Temperature	Max Temp, Min Temp (Observed)	BMD	BMD stations	Monthly	2000–2022
	ECMWF ERA5	Copernicus C3S	0.1 ° X0.1 °	Monthly	2000–2022
PET	Total PET (Observed)	BMD	BMD station	Monthly	2000–2022
Land Cover	MCD12Q1 V6	NASA LP DAAC	500 m	Yearly	2001–2022

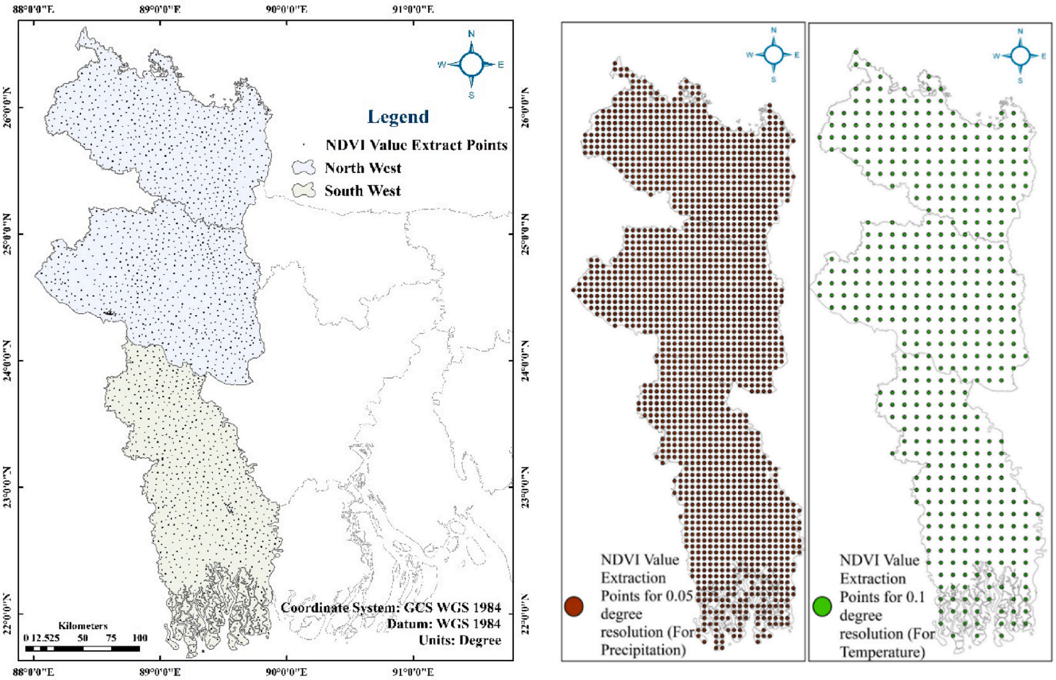

Fig. 2. NDVI value extraction points for various analysis. Fig. 2(a) shows NDVI extraction points for each union and Fig. 2(b) denotes NDVI extraction points with 0.05-degree resolution and Fig. 2(c) shows NDVI extraction points for 0.1-degree resolution.

temperature data were used to correlate with NDVI through correlation mapping. Land use maps were generated to derive the areas of different types of land use and the values were correlated with yearly average NDVI values of the region with Pearson Correlation method.

2.4.1. Spatial auto-correlation of NDVI values

Spatial autocorrelation is used to assess the presence of systematic spatial variation in a mapped variable [99–101]. In this study, Moran's I Statistics and Getis Ord Gi* were adopted for the purpose of visualizing the spatial distribution of NDVI values of dry season (November–February) in the region and the relationship of each NDVI pixels with its neighboring grids. For this analysis, NDVI of drier months were employed for dual reasonings and they are-

1. The lack of constant availability of NDVI values during the monsoon season,
2. The first limitation arises due to the annual monsoon flooding occurrences which impede the acquisition of correct NDVI values from the region.

Moran's I is one of the widely used global index of spatial autocorrelation to measure the similarity of values in neighboring places from a mean value [102]. A positive Moran's I index value would indicate tendency toward spatial clustering, while a negative value would indicate tendency to disperse while a value close to 0 would represent complete spatial randomness.

Moran's I only measure the overall spatial autocorrelation as it does not distinguish between positive and negative spatial auto-correlation or capture the spatial arrangement of neighboring values. Hence, Getis Ord Gi* were conducted in this study.

Getis-Ord G_i* is a hot-spot analysis tool for spatial autocorrelation where the resultant z-scores and p-values determine if the spatial features are either clustered or not [103,104]. Here, positive G_i* statistics with high absolute values correspond to clusters with high-value events and negative G_i* statistics with high absolute values correspond to clusters with low-value events.

2.4.2. Temporal correlation of NDVI values

For examining the existence of increasing or decreasing patterns in the NDVI values of each district in the study regions, two methods were applied –

1. Mann Kendall and Sen's slope test and,
2. Innovative Trend Analysis (ITA)

The Mann-Kendall (MK) statistical test is a rank-based non-parametric test of detecting trends in various hydrometeorological times series [105]. Sen's slope is the nonparametric estimate of the slope for the set of pairs (i, X_i) where X_i is a time series [106].

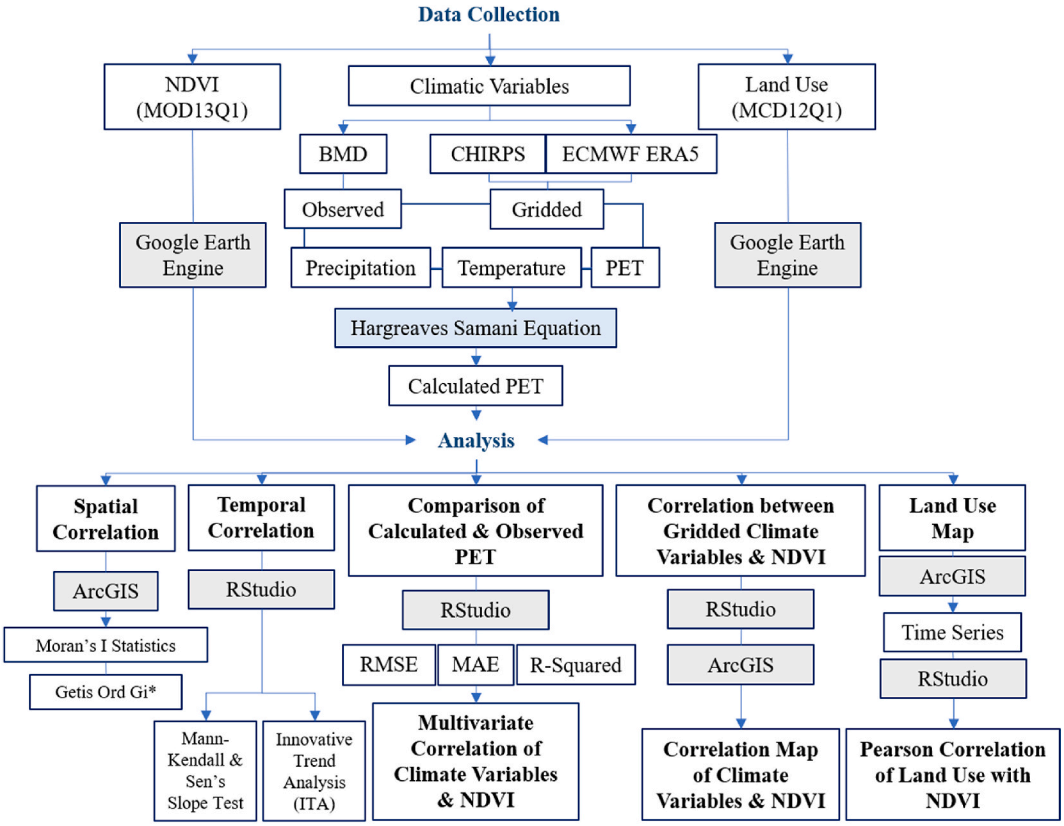

Fig. 3. Methodology of the study. This figure elaborates the data collection and pre-processing processes along with different analysis methods deployed in the study.

If Mann-Kendall statistics is defined as S [107],
then S is defined as follows:

$$S = \sum_{i=1}^{n-1} \sum_{j=i+1}^{n} sgn(X_j - X_i)$$

where the X_j are the sequential data values, n is the length of the time series, and

$$\mathrm{sgn}(\theta) = \begin{cases} 1 \; if \; \theta > 0 \\ 0 \; if \; \theta = 0 \\ -1 \; if \; \theta < 0 \end{cases}$$

Mann and Kendall have documented that the statistic S is approximately normally distributed when $n \geq 8$, with the mean and the variance of statistics S as follows:

$$V(S) = \frac{n(n\text{-}1)(2n+5)\text{-}\sum_{i=1}^{n} t_i i(i-1)(2i+5)}{18}$$

where, t_i is the number of ties of extent i, n is the number of groups of tied ranks. The standardized test statistic Z is computed by,

$$Z = \begin{cases} \dfrac{S-1}{\sqrt{Var(S)}} \; ; S > 0 \\ 0 \quad ; S = 0 \\ \dfrac{S+1}{\sqrt{Var(S)}} \; ; S < 0 \end{cases}$$

$$\mathrm{p} = 0.5 \; - \; (|\mathrm{Z}|)$$

$$\varnothing(|Z|) = \frac{1}{\sqrt{2\pi}} \int_0^{|Z|} e^{-\frac{t^2}{2}}\, dt$$

Z follows the standard normal distribution with $E(Z) = 0$ and $V(Z) = 1$, and the null hypothesis is rejected if the absolute value of *Z* is larger than the theoretical value $Z_{1-\alpha/2}$ (for two-tailed test) or $Z_{1-\alpha}$ (for one-tailed test).

Here, α = the statistical significance level.

Moreover, Sen's slope is defined as,

$$Sen'slope = Medium \left\{ \frac{X_j - X_i}{j - i} \right. ; i < j$$

A (1–α) confidence interval for Sen's slope can be calculated as (lower, upper) where

$$N = C\,(n, 2)\ k = se \cdot z_{crit}$$

$$lower = m_{(N-k)/2}\ upper = m_{\{(N+k)/2\}+1}$$

here,

N = the number of pairs of time series elements (x_i, x_j) where $i < j$, se = the standard error for the Mann Kendall test, m_h = the hth smallest in the set $\{\frac{X_j - X_i}{j-i}: i < j\}$ and z_{crit} = the $(1-\frac{\alpha}{2})$ critical value for the normal distribution.

There are two hypothesis of Mann Kendall test and they are-the null hypothesis associated with higher p-values ($p > 0.05$) and low z-values; when there is no monotonic trend in the series and the alternate hypothesis associated with lower p-values ($p < 0.05$) and high z-values when there exists a trend. A positive value of *Z* indicates a positive trend and negative value of *Z* indicates a downward trend.

Though Mann-Kendall has been proved to be strong trend detector in various studies, to assess whether non-monotonic trend exists in the NDVI patterns of the study regions and to free the trend results from Mann Kendall Test's assumptions, Innovative Trend Analysis was also utilized in this study.

The Innovative Trend Analysis (ITA) is a non-parametric method to detect monotonic, non-monotonic and sub-trends in time series datasets through graphical presentation [108]. In this method, first the time series is divided into two equal parts and sorted in ascending order. The first and second half of the time series are places on the X-axis and Y-axis of the graph respectively. Then, a 1:1 ideal line (45° line) is drawn within the graph. If the data plotted are on the 1:1 line, there exists on trend in the concerned time series. If the data are located on the upper triangle of the ideal line, there exists an increasing trend. Similarly, data points on the lower triangular area suggests a decreasing trend [83].

2.4.3. PET calculation

In regions where meteorological variables are scarce, the Hargreaves-Samani (HS) equation is used to calculate Potential Evapotranspiration (PET) [109] as it needs less climatic data as variables [110–112]. In this study, observed PET data from BMD were not continuous from 2000 to 2022 for all BMD stations, hence, Hargreaves-Samani equation were utilized to calculate PET.

According to Hargreaves Samani PET equation,

$$PET = 0.0023 R_a\, (T_{max} - T_{min})^{0.5}\, (T_{mean} + 17.8)$$

where, *PET (mm/day)* = Potential evapotranspiration, R_a = Mean extra-terrestrial radiation in mm/day which is a function of latitude, T_{max} = Maximum daily air temperature in ^{O}C, T_{min} = Minimum daily air temperature in ^{O}C, T_{mean} = Average daily air Temperature in ^{O}C

In this method, the extraterrestrial radiation (R_a) is estimated using the following equation,

$$R_a = \frac{24(60)}{\pi} G_{sc}\ d_r\, [\omega s \sin(\varnothing)\sin(\delta) + \cos(\varnothing)\cos(\delta)\sin(\omega_s)$$

where, R_a is extraterrestrial radiation [MJ m^2 day^{-1}], G_{sc} is the solar constant = 0.0820 MJ m^2 min^{-1}, d_r is the inverse relative distance Earth–Sun, ω_s is the sunset hour angle [rad], φ is latitude [rad], and δ is solar declination [rad].

The inverse relative distance Earth–Sun, $d_r = 1 + 0.033 \cos\left(\frac{2\pi}{365} J\right)$.

and the solar declination, $\delta = 0.409 \sin\left(\frac{2\pi}{365} J - 1.39\right)$.

where, J is the number of the day in the year between 1 (01 January) and 365 or 366 (31 December).

The sunset hour angle, $\omega_s = \arccos[-\tan(\varnothing)\tan(\delta)]$.

2.4.4. RMSE, MAE, R-squared values to compare calculated and observed PET

Calculated PET was assessed against available observed PET values using RMSE, MAE and R-squared values to check its efficacy as a replacement of the observed values in subsequent analysis.

Root Mean Square Error (RMSE) is a performance indicator which measures the average difference between values predicted and the actual values. Here,

$$\mathrm{RMSE} = \sqrt{\frac{\sum_{n=1}^{N}\left(\hat{r}_n - r_n\right)^2}{N}} \text{ [113]}$$

where $\hat{r}_n$ means the observed data; r_n means the climate model data, N is sample size.

Mean Absolute Error (MAE) is a measurement of errors between two sets of datasets of the same variable [114]. The formula is as follows:

$$MAE = \frac{\sum_{i=1}^{n}|y_i - x_i|}{n} = \frac{\sum_{i=1}^{n}|e_i|}{n}$$

There is no agreement on a standard range of values for RMSE and MAE. The smaller the value of RMSE and MAE, the better the similarity of the calculated value with their observed counterparts [115].

R-Squared or R^2 is a statistical measure that shows how linearly related two random valuables are [54]. The value ranges from 0 to 1. The similar the calculated values are to the observed values, the closes its R^2 will be to 1. A value less than 0.2 indicates no correlation, between 0.2 and 0.4 denotes small correlation, 0.4 to 0.7 results in moderate correlation and greater than 0.7 translated to strong correlation.

2.4.5. *Multivariate correlation analysis*

The multivariate analysis finds patterns and correlates between several variables simultaneously. In this study, the monthly total precipitation, monthly average minimum temperature, monthly average maximum temperature, monthly potential evapotranspiration from 2000 to 2022 were correlated as climatic variables against Monthly average NDVI values for the 11 BMD stations situated in the study regions.

2.4.6. *Correlation mapping of gridded climate data with NDVI*

Acquiring NDVI values corresponding to the CHIRPS and ECMWF ERA5 data for each month for the region ensured a nuanced dataset with each grid possessing an extensive repository of monthly precipitation and NDVI values, monthly mean temperature with NDVI values for 23-year period from 2000 to 2022. The correlation coefficient analyses were executed for each grid. Computed correlation coefficients were subsequently employed to generate the correlation maps where each grid of the map had one corresponding value assigned for both NDVI-Precipitation and NDVI-temperature correlation maps.

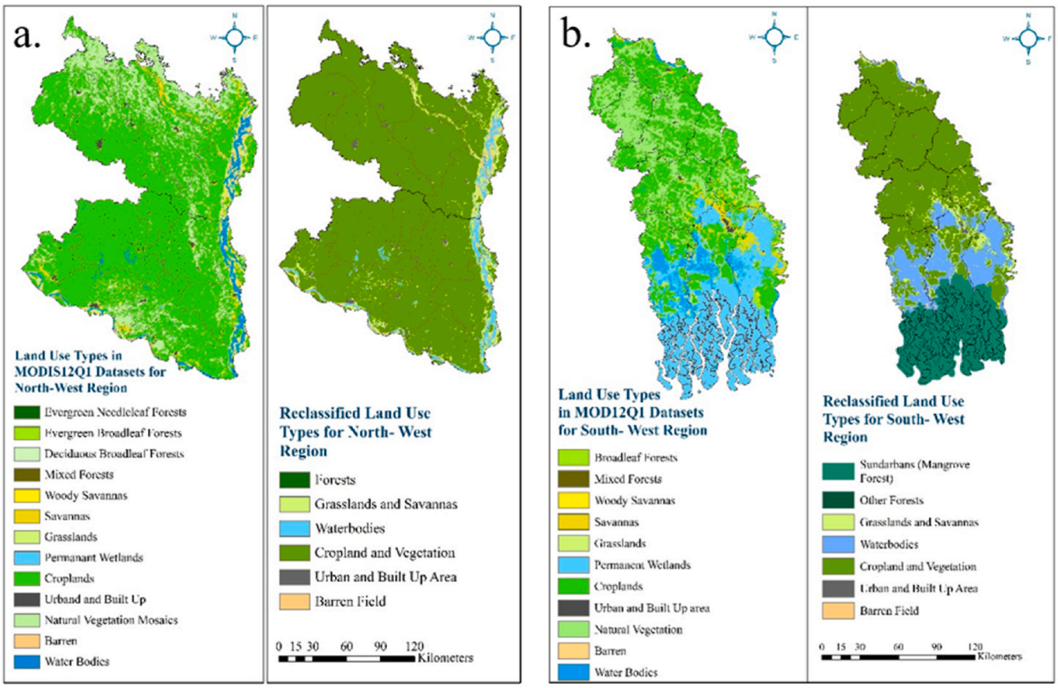

Fig. 4. Visualization of Land Cover Reclassification of a. North-West and b. South-West region. There were 13 initial land use types available in MCD12Q1 datasets for the study regions. They were classified into 6 land cover types - Forests, Grassland and Savannas, Waterbodies, Cropland and Vegetation, Urban and Built Up area and Barren Field for the North-West Region. For South-West region, Sundarbans is shown in a different land cover types because of their mangrove nature which is different than other forest areas in the region.

2.4.7. Land cover and NDVI trend analysis with Pearson Product Moment Correlation

There were 17 different classifications in MCD12Q1 dataset for land use and out of them, 13 were available for the study regions. These were converted into 6 types of land use in North-West including Forests, Grassland and Savannas, Waterbodies, Cropland and Vegetation, Urban and Built-up area and Barren field and 7 types of land use in South-West. For South-West region, one additional land

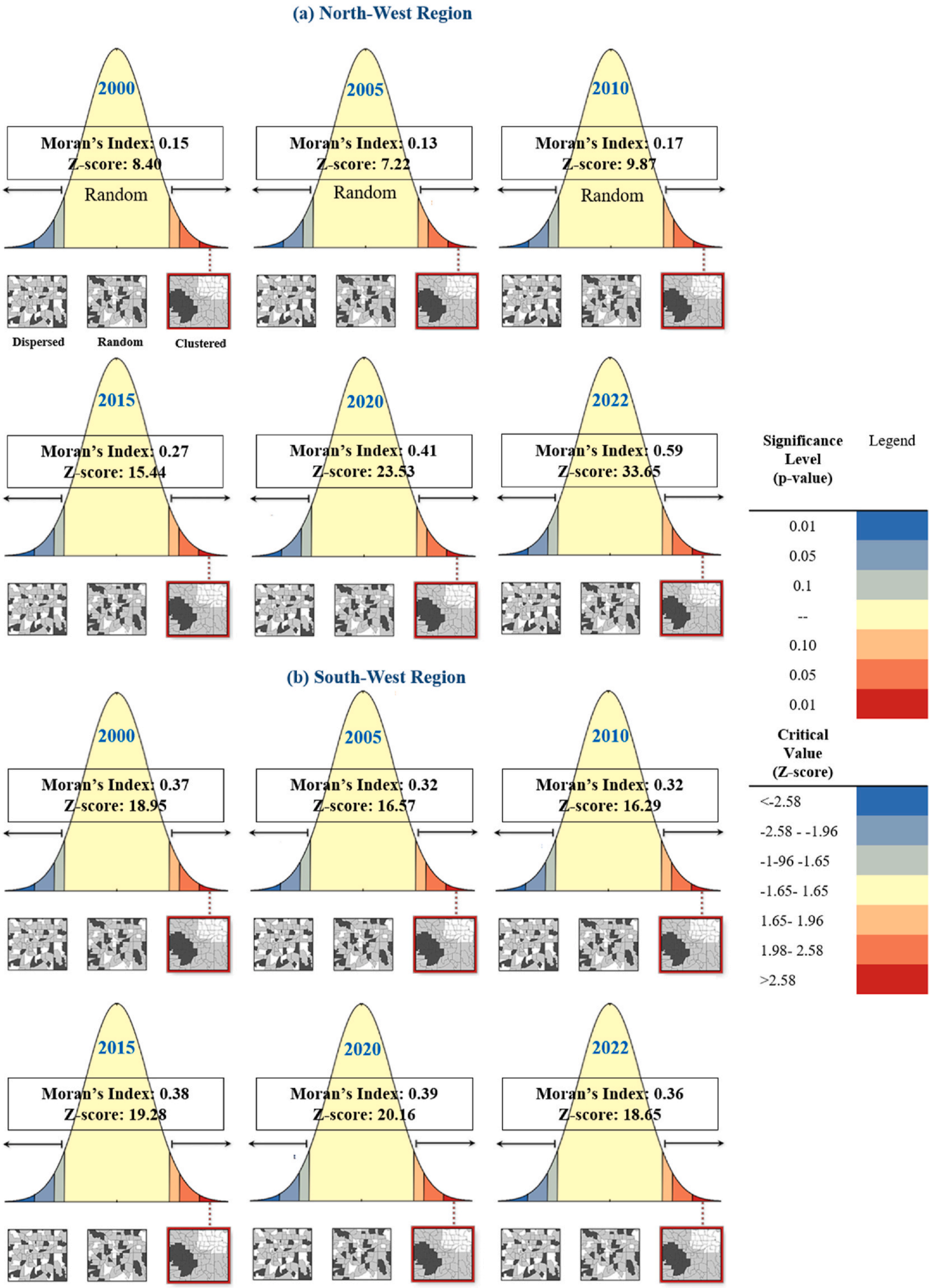

Fig. 5. Moran's I Statistics Results of NDVI spatial autocorrelation for (a) North-West and (b) South-West Region. For both regions, the p-values are less than 0.05 and critical Z-values are greater than 2.58. This means the NDVI values are spatially clustered for the regions from 2000 to 2022.

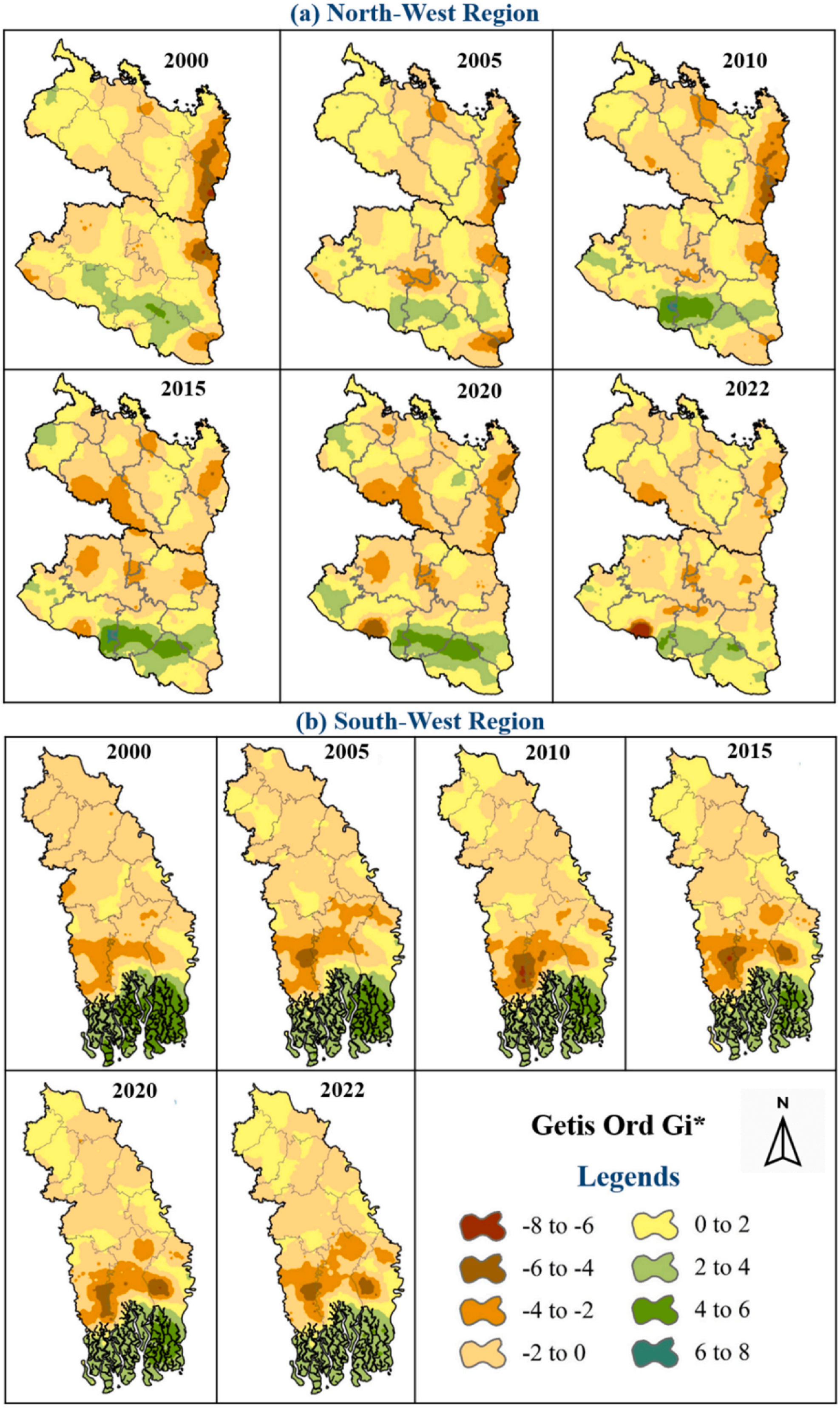

(caption on next page)

Fig. 6. Inverted Distance Weighted Maps for Getis Ord Gi* Analysis of NDVI values for (a) North-West & (b) South-West regions. High cold-spots (Low NDVI clusters) are denoted with red and high hotspots (High NDVI clusters) are denoted with red and high hotspots (High NDVI clusters) are denoted with green in the maps. And moderate, low and neutral clustered zones are visualized by the color spectrum in between.

use types, Sundarbans, Mangrove Forest was added. The reclassifications are shown in Fig. 4(a) for North-West region and Fig. 4(b) for South-West region respectively.

Pearson Product Moment Correlation was used to assess the changes in different types of reclassified land use over the period of 22 years and its correlation with the changes of NDVI values of the region. It is one of the most common ways of measuring linear correlations between two environmental, hydrological or land use/land cover variables [116,117]. Here, correlations were assessed based on the changes of Forests, Cropland and vegetation, Grassland, Barren Field areas with the monthly Average NDVI values changing for all three divisions in both NW and SW regions.

3. Results

3.1. Spatial and temporal variation of NDVI values

3.1.1. Spatial distribution and clustering trend of NDVI values

The results of Moran's I statistics based on dry month (November–February) NDVI values in Fig. 5(a) for North-West region and Fig. 5(b) for South-West region, suggested that the p-values associated with the spatial correlation values are less than 0.05 for all considered years- 2000, 2005, 2010, 2015, 2020 and 2022 whereas the critical Z-value are greater than 2.58 for all instances. This determines the presence of spatial autocorrelation, thereby determining the patterns of NDVI values have been clustered in the study region over the years. For NW, the Moran's Index values as well as Z-values are rising since 2000 which signifies that the spatial correlation is increasing over the last 23 years in NW. However, for SW, the values show a slight decrease in 2005 and 2010 from 2000, and a small increase in the next years implying the spatial correlation has largely been steady in SW.

Getis Ord Gi* analyses were done and the results were denoted by IDW Method as shown in Fig. 6(a) for North-West and Fig. 6(b) for South-West regions. The result showed that the southern part of the NW region has had hotspot zones throughout the years meaning high NDVI value zones are adjacent to each other in this region. The eastern part of the NW region has been changing from a cold spot to a statistically insignificant neutral zone. For SW, the lower part of region has shown high clustered values. This is because of the Sundarbans, the mangrove forest that is situated in this part of the region. The dense forest attributed to the high clustering in that zone with higher NDVI values denoting it as a hotspot for Getis Ord Gi* analyses. The upper part of the SW region has been slowing down its cold spots changing into a more neutral zone over the 23-year study period indicating an increase of vegetation greenness in the region.

3.1.2. Time series analysis of temporal changes in NDVI values

Time series plotting for all 26 districts of the study region are given in Appendix A. The trends are upwards. Correspondingly, Mann Kendall test results derived from the time series values shown in Table 2 point out that the changes in the monthly NDVI values for 2000 to 2022 were significant for all 26 districts as the p-values were less than 0.5 with z values being greater than 1.96. The positive Tau value of Mann Kendall test and upward value of Sen's slope indicate that NDVI values were increasing for all the districts.

The ITA results for the districts express similar results showing positive slope values as shown in Fig. 7(a–z). In these graphs, the upper triangle is the increasing trend region for NDVI values and the lower triangle is the decreasing trend region. The graphs illustrate that the datapoints for all 26 districts reside in the upper triangle. In light of this, the conclusion is reached that for all of the regions NDVI values are increasing for the 23-year period of 2000–2022. Accordingly, the plots show that the NDVI values are in monotonic increasing trends as data points do not cross the 1:1 no trend lines in any instances and never do in the decreasing trend region for any of the districts. Only the district of Panchagarh has some datapoints on the 1:1 no-trend line which is overshadowed by the large portion of the dataset being on the increasing side. This is similar with the results derived from Mann-Kendall and Sen's slope test results for the same districts.

3.2. Efficacy of calculated PET values in comparison with observed PET values

RMSE, MAE and R^2 values for comparing calculated PET with observed PET for all 11 BMD stations are shown in Fig. 8(a–k). The RMSE values are in the range of 0.50–0.75, MAE values are from 0.40 to 0.58 which means the error values in these two considerations are minimal. Additionally, R^2 values are greater than 0.70 in all instances, suggesting strong similarity of the calculated PET with observed PET. Hence, the calculated PET values are similar to the observed values in terms of values and similar trends with minimal error values.

Table 2
Mann Kendall and Sen's Slope Test Results for All 26 districts in North-West and South-West region.

Mann Kendall Test Results						Sen's slope results
p-value	*Hypothesis*	*Significance*	*Z value*	*Tau value*	*Trend*	*Trend*
<0.05	Alternative	Significant	>1.96	Positive	Increasing	Upward

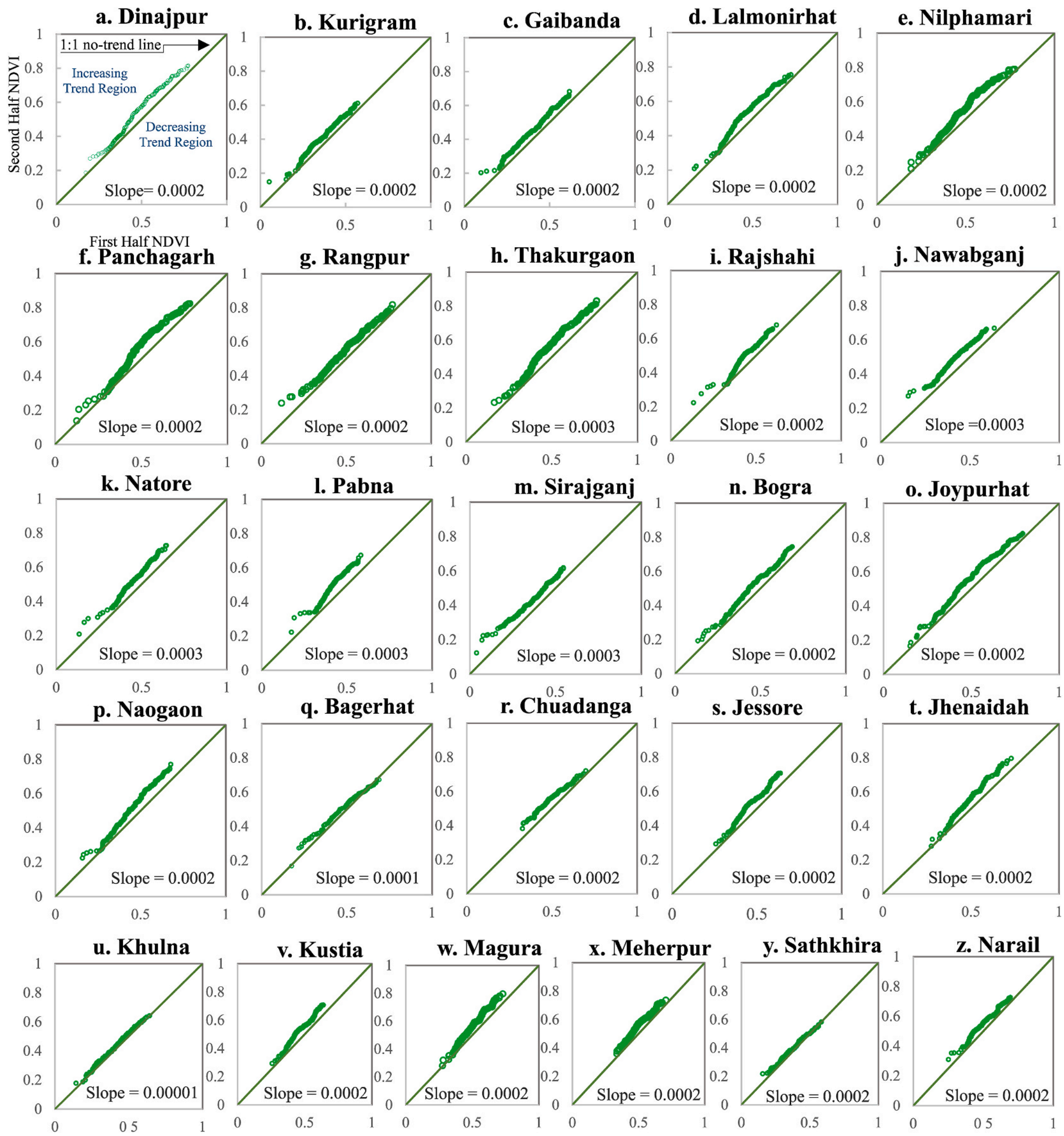

Fig. 7. Innovative Trend Results for all 26 districts in the North-West and South-West of Bangladesh. For all the plots, datapoints reside in the increasing trend region (Displayed in the first graph for Dinajpur) signifying the increment of NDVI values in the study region.

3.3. Multivariate correlation of NDVI with observed and calculated climatic variables

The plotting for multivariate correlation matrices for the 11 BMD stations, as per Table 3, showed no climate variable being particularly dominant with NDVI changes in the region. The multivariate plot for Rajshahi BMD station is displayed in Fig. 9 with rest of the BMD stations displayed in Appendix B. Some of the stations showed slight to moderate correlation for the climate variables, but no correlation showed any definite pattern. In comparison to other climate variables, temperature has shown some amount of slight and moderate correlations for the BMD stations of the study region.

3.4. Correlation of NDVI values with gridded precipitation and temperature data

The temperature-NDVI correlation map showed varying degrees of correlation between the two variables as shown in Fig. 10, Where mostly slight correlation was pertinent between temperature and NDVI values for BMD stations, the correlation mapping from gridded datasets results showed stronger positive and negative correlation between temperature and NDVI values throughout the regions.

The time series of monthly mean temperature in Fig. 11(a) and NDVI in Fig. 11(b) for the Sundarbans were analyzed. The trends showed that the NDVI values of the region kept increasing at a subtle rate, but the temperature trend showed virtually no change. So,

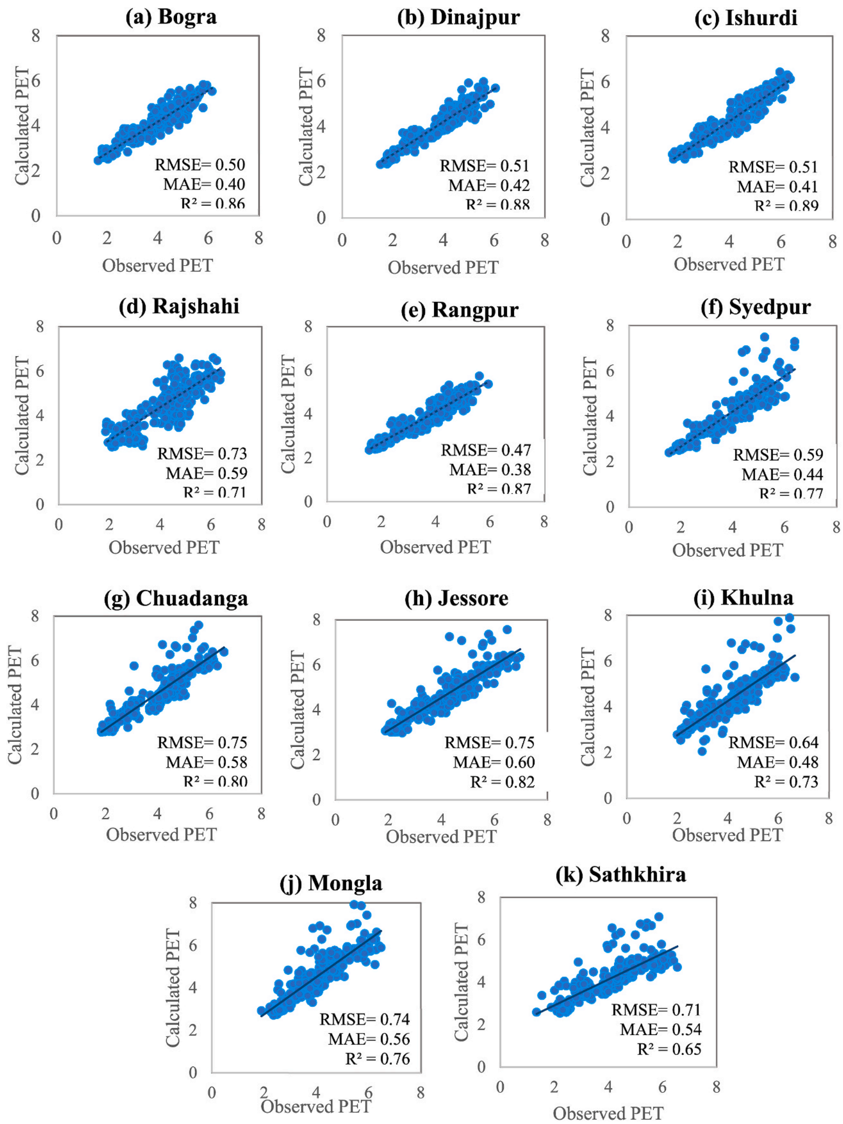

Fig. 8. Comparison of Calculated and Observed PET values for the BMD Stations. RMSE and MAE values for all the stations are below 1, while R-squared values are greater than 0.7 for the same. The values suggest that the calculated PET are comparable to observed PET values for the stations.

Table 3
Multivariate correlation results of NDVI and climate variables for the BMD stations.

BMD Stations	Precipitation	Max Temp	Min Temp	PET
Bogra	0.19	0.33	0.29	0.15
Dinajpur	0.14	0.43	0.38	0.23
Ishurdi	−0.32	0.26	−0.12	0.44
Rajshahi	0.07	0.21	0.22	0.05
Rangpur	−0.06	0.19	0.19	0
Syedpur	0.08	0.39	0.33	0.19
Chuadanga	−0.04	−0.34	−0.34	−0.3
Jessore	−0.01	0.23	0.18	0.08
Khulna	0	0.14	0.25	−0.11
Mongla	−0.5	−0.25	−0.42	−0.3
Sathkhira	−0.04	−0.07	−0.02	−0.2

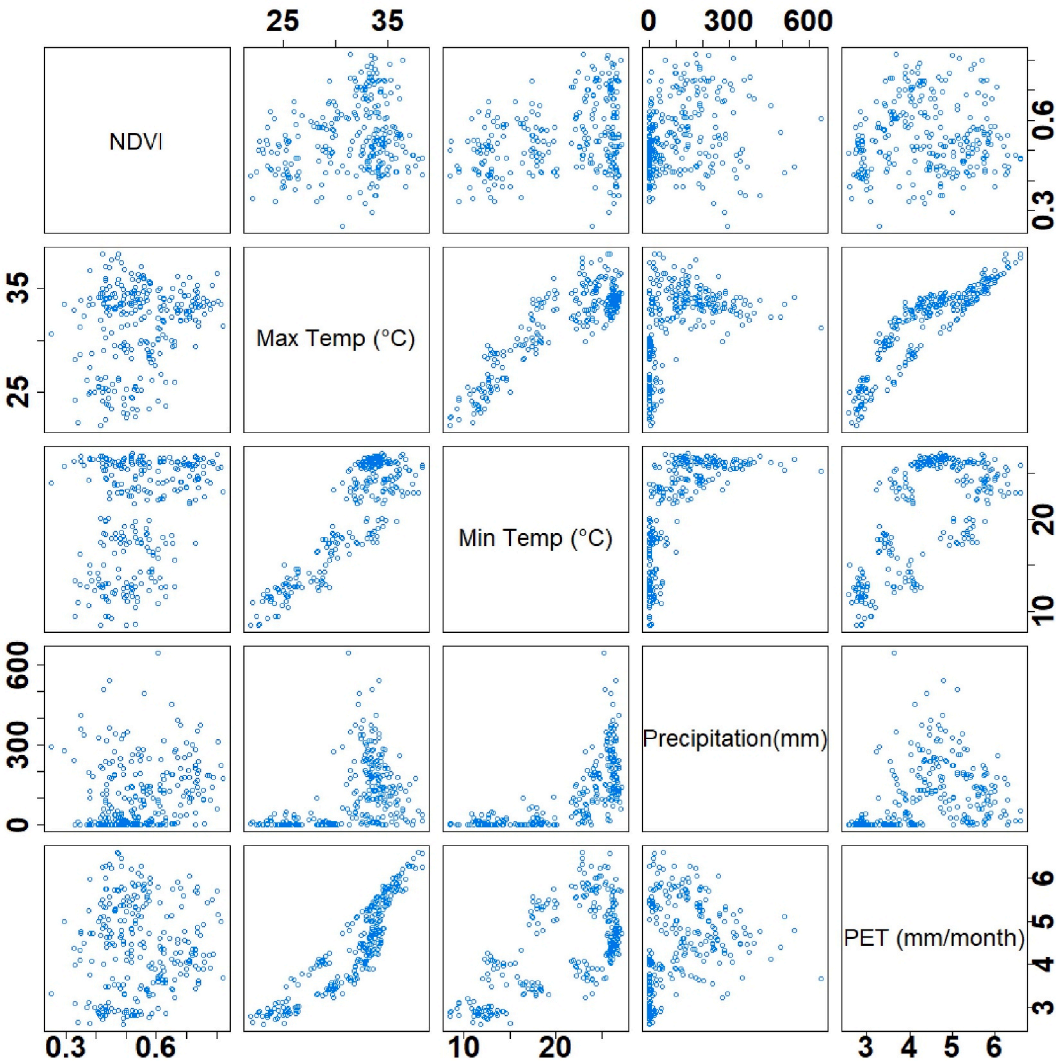

Fig. 9. Multivariate correlation plot of NDVI, monthly total precipitation, monthly maximum and minimum temperature, monthly total PET for Rajshahi BMD Station.

the correlation between temperature and NDVI showed moderate negative correlation for the Sundarbans area.

3.5. Correlation between land cover changes and NDVI patterns

From the land use maps generated from 2001 to 2022, portrayed in Appendix C. Time series analyses were done for various land types- Forest, Grassland, Barren field and Cropland, along with yearly average NDVI values. Time series trends for South-West (Khulna Division) is shown in Fig. 12 and (a) for forest area, Fig. 12(b) for Grassland, Fig. 12(c) for Barren field, Fig. 12(d) for Grassland and Fig. 12(e) for yearly average NDVI of South-West region. Likewise, time series trends for North-West (Rajshahi and Rangpur Division) are portrayed in Appendix D.

Time series plots showed that Grassland and barren field areas decreased with time for all divisions but cropland and vegetation areas increased for the study period. Additionally, for SW region, the forest area showed an increasing trend. At the same time, the yearly average NDVI values also increased for all three divisions of NW and SW regions.

The trends for different land use types were then correlated with average yearly NDVI values through Pearson Product Moment Correlation as shown in Table 3. Both NW and SW regions had positive correlations of NDVI with cropland and vegetation area and negative correlation with Grassland and Barren area. Additionally, for SW, Forest also showed positive correlation against NDVI. These values showed that both NW and SW region have had significant land cover changing from land types with lower NDVI values to land types with higher NDVI values.

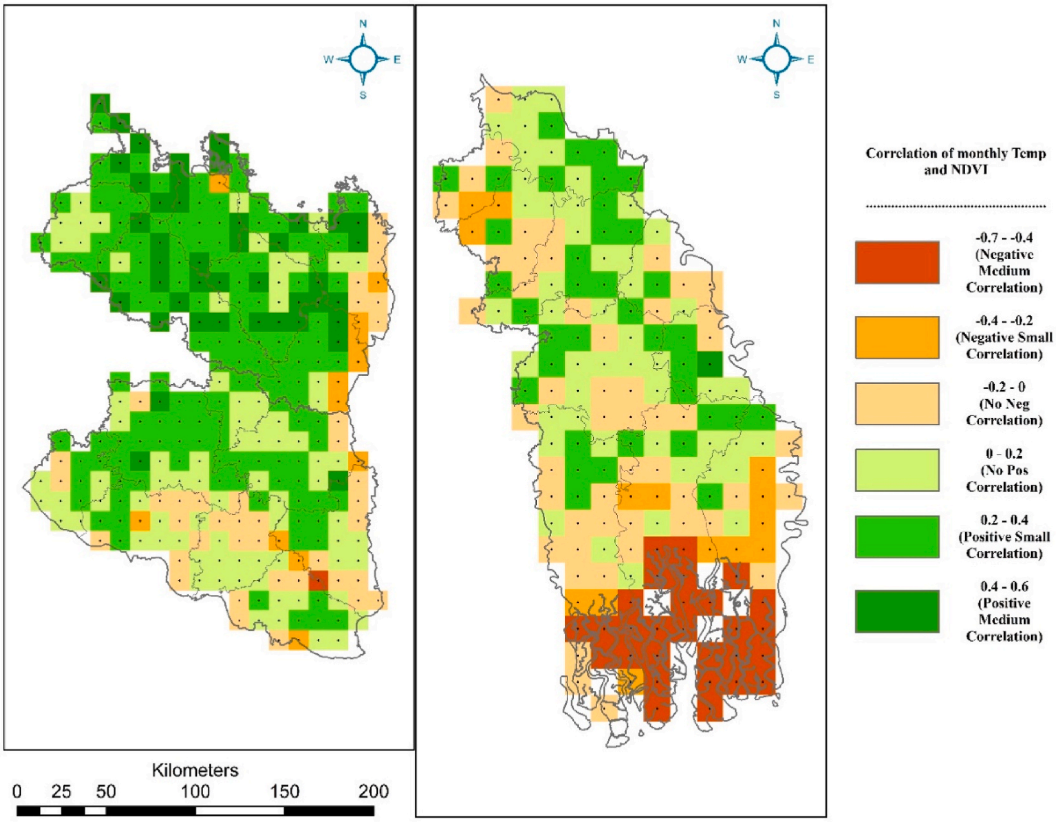

Fig. 10. Correlation Map of Monthly mean temperature and NDVI map for (a)North-West and (b)South-West regions. The correlation between temperature and NDVI ranges from strong negative correlation (denoted by red) to medium positive correlation (denoted by green).

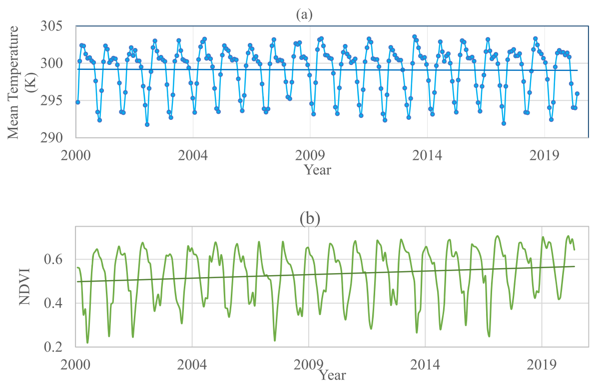

Fig. 11. Time series for (a)Mean Temperature and (b)NDVI values for the Sundarbans. The trend in mean temperature shows no virtual upwardness whereas the NDVI trend shows that the values are going upwards throughout the years.

4. Discussion

The findings of Moran'I Statistics reveal a consistent pattern of dry month NDVI values clustering within specific regions over the 23-year study period where it is seen that the clustering phenomena is increasing in the NW compared to SW of Bangladesh. This suggests that over an extended timeframe, the nature of vegetation dynamics within these areas are persistent and stable. However, Moran's I could not show where the positive and negative values are clustered in the study area. Getis Ord Gi* alleviates this constraint, thereby demonstrating the high NDVI and low NDVI clustered zones. Both regions show that most of the areas are cold spots or neutral zones, thereby showcasing the dominance of low NDVI areas in the regions over the years. Nevertheless, the southern part of NW has seen an increase of high clustered zones from 2000 to 2020, with slight reduction in 2022. This shows that vegetation greenness and

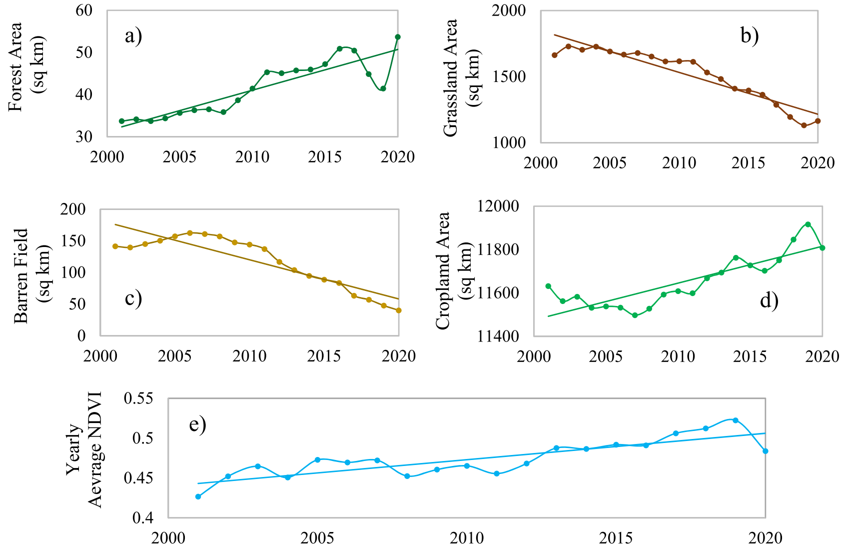

Fig. 12. Trends of a) Forest area increasing, b) Grassland area decreasing, c) Barren Field decreasing, d) Cropland area increasing, e) Yearly average NDVI increasing from 2001 to 2020 for Khulna (SW).

areas are more persistent in southern NW, under Rajshahi division. Moreover, the results interpret that the high cold spots are changing towards neutral zones towards the eastern part of NW in Rangpur division, which suggest that vegetation greenness in terms of area is increasing over the years. This indicates small expansion of crop and vegetation area in NW over the last 23 years. In SW, the findings persist unchanged scenarios of cold spots for most areas with high-NDVI value zones in the Sundarbans area, which has been densely forested because of the existence of the Mangrove forest. Hence, spatially NW and SW, being drier regions of Bangladesh, did not have overwhelming expansion of high NDVI zones in the mentioned time frame. Nonetheless, the changes made in NW are noteworthy because the identified areas are closer to two big rivers-the Jamuna and the Padma, suggesting the existence of water sources nearby has the potential to transform the drier regions in a greener state, even in the dry season. Moreover, the Mann Kendall test indicates a statistically significant upward trend in NDVI values which is further corroborated by Sen's slope values. However, to mitigate any inherent assumptions made in the Mann-Kendall test and to ascertain whether the trends are monotonic or not, Innovative Trend Analysis (ITA) was undertaken. This affirmed that the observed trends are indeed monotonous and so validating the findings from the Mann-Kendall test as Mann-Kendall test is effective in detecting monotonic trend. On top of that, the ITA based plots reinforce the previously obtained results of NDVI values exhibiting consistent upward trend across all 26 districts spanning from 2000 to 2022. Comparing the temporal trend results with spatial correlation results, it can be derived that although the changes in NDVI values in the region are not yet sufficient to alter the spatial distribution of NDVI clustering zones prominently, the NDVI values are still increasing all over the region with time.

Furthermore, the study show no particular relationship pattern emerges between NDVI and climate variables for the 11 BMD stations over the study period of 23 years through Multivariate correlation. However, only assessing 11 BMD station for two hydrological and dynamic regions are insufficient to conclude with this assessment. Correlation Mapping with more defined resolution could mitigate this limitation and so correlation mapping of NDVI-Precipitation and NDVI-temperature was conducted. The NDVI-precipitation map for the entire region showed virtually no significant correlations between the two variables for the study region even at 0.05 ° grid. It corresponds to the multivariate correlation results where observed precipitation did not show strong correlation with NDVI values for the BMD stations. On the Contrary, temperature-NDVI maps showed significant improvement in results denoting that the average temperature and the increasing NDVI values are correlated with each other throughout the region when considering these two variables for 23 years. There have been distinct differences between the correlation results between NW and SW region. NW has shown significantly more positive correlation with only a few grids showing no correlation or slight negative correlation. This means at 0.1 °, temperature has had higher impact on the NDVI values for the NW region. On the other hand, SW has shown both positive and negative correlations. The North-eastern part of the SW region has shown the most areas with positive correlation; this means temperature is significant for NDVI value fluctuations for the North-eastern part of SW region. From going north to south in SW, the correlation values shifted towards more neutral and negative correlation values with distinct negative correlation towards the southern part of Khulna division. This area encompasses the Sundarbans, the mangrove forest. Hence, this alerted the need for further assessment for this particular region. Upon inspecting further, it was evident that the temperature in the Sundarbans region are stable over the concerned years with an increment in NDVI values which prompts of the results of negative correlation values in the particular region. This finding is intriguing because it shows the temperature trends in the Sundarbans are different than the other parts of NW and SW, which are historically drier hydrological regions, especially when this is the only densely forest zone in the study area.

This prompted the need of subsequent inquiry about the contribution of land cover types in NDVI. Pearson product moment correlation analysis for the significant land cover types were then deployed for this purpose. The finding revealed that the types of land cover and their changing patterns have apparent strong influence on the vegetation greenness in all parts of the regions. The changing patterns of land cover types from 2001 to 2022 posits that the expansion of agricultural activities and vegetation production which triggered the land cover to transmute from barren field and grassland into cropland is a prominent contributor in augmenting the verdancy in NW and SW of Bangladesh. The drastic changes in correlation results observed from altering the spatial resolution of climatic variables from only 11 BMD stations to taking data points by each $0.1^{\circ}X0.1^{\circ}$ resolution makes the spatial resolution of the datasets used in the research a critical aspect to address. It shows that the ability to detect and analyze spatial patterns and changes is directly dependent on the spatial scale used. Datasets with coarser spatial resolution used in the study such as MODIS NDVI (MOD13Q1) and land cover (MCD12Q1) could pose a possibility of missing or masking more nuanced or localized changes. However, for analyzing regional climatic trends and land cover changes, datasets used in coarser spatial resolution can still prove to be as much valuable if the area tends to be more of surrounded with homogeneous landscapes which is for the cases of NW and SW of Bangladesh. Furthermore, spatial and temporal high-resolution data like ESRI Sentinel Land cover datasets could have proven to be more valuable incorporating the localized changes. But they have only been made available from 2017 which limits its usage in long time analyses like this study. On top of that, the higher spatial resolution of the datasets, if used, would have needed greater computational resources and processing time limiting the extent and depth of the analyses and introducing more data biases.

The findings of the study suggest the contention that the vegetation density, greenness and spatial extension of vegetation are closely linked with alterations in land cover, driven by anthropogenic activities like crop production or farming rather than being exclusively dictated by the changes in climatic variables for the NW and SW regions of Bangladesh. These results can be counter-intuitive and so they can provide the basis of exploring the natural and man-made factors for increasing vegetation in previously less vegetative regions. This is particularly important for agricultural dependent regions like Bangladesh because the expansion of vegetation greenness through various agricultural activities and food production methods prerequires the appropriate changes of climate patterns and land cover changes favorable to the condition. Hence, similar studies incorporating more climatic variables covering different hydrological regions of Bangladesh can help make a comprehensive picture of vegetation health and greenery in Bangladesh considering different geological and hydrological factors.

5. Conclusion

The study primarily focused on exploring the spatial and temporal distribution and trends of NDVI values and their correlation with climatic parameters alongside the dynamics of land cover changes in the North-West (NW) and South-West (SW) regions of Bangladesh spanning over 23 years, from 2000 to 2022. The analyses indicated that the historical drought prone zones of Bangladesh, NW and SW, have been shifting towards having increased NDVI values spatially and temporally in the drier months of the years, November–February. For the 11 meteorological stations present in the regions, climate variables such as precipitation, maximum and minimum temperature and PET did not show any dominate or significant correlation pattern with the overall increasing NDVI values. When the correlation analysis with gridded precipitation and temperature variables were carried out, correlation mappings showed that temperature trends have significant correlation with increasing vegetation indices values when the analysis was done in finer resolution of 0.1° resolution, but precipitation showed almost no correlation even at a finer resolution of 0.05°. Lastly, changes in all significant land cover types present in the regions showed moderate to strong correlation with NDVI values increasing. The land covers changing patterns for both regions showed expansion in cropland and vegetation areas along with contraction of barren field and grassland over the study period. Hence, the investigations showed that land cover changing to crop areas or agricultural fields from grassland, barren fields and fallow lands have been the more dominant fact for the increment of NDVI values in the regions comparing with climatic variable trends.

6. Data availability statement

The data used in the study were collected from multiple sources. They are mentioned below:

- The NDVI data are available in a dataset from Google Earth Engine Data Catalog named MOD13Q1.061 Terra Vegetation Indices 16-Day Global 250 m (https://developers.google.com/earth-engine/datasets/catalog/MODIS_061_MOD13Q1).
- The observed climatic data used for the BMD stations are available in a Bangladesh Agricultural Research Council Website named Climate Information Management System (Precipitation data is available at http://barcapps.gov.bd/climate/rainfall, Temperature data is available at http://barcapps.gov.bd/climate/temp, PET data is available at http://barcapps.gov.bd/climate/pet).
- climatic datasets- CHIRPS for Precipitation are available, in the website of Climate Hazards Center, UC Santa Barbara, here- https://data.chc.ucsb.edu/products/CHIRPS-2.0/and ECMWF ERA5 for Temperature are available in Copernicus Climate Change Service website (ERA5-Land monthly averaged data from 1950 to present- https://cds.climate.copernicus.eu/cdsapp#!/dataset/reanalysis-era5-land-monthly-means?tab=form).
- The Land Cover dataset is available at Google Earth Engine Data Catalog named MCD12Q1.061 MODIS Land Cover Type Yearly Global 500 m, available at https://developers.google.com/earth-engine/datasets/catalog/MODIS_061_MCD12Q1.

CRediT authorship contribution statement

Jumana Akhter: Writing – review & editing, Writing – original draft, Visualization, Software, Methodology, Formal analysis, Conceptualization. **Rounak Afroz:** Writing – review & editing, Supervision, Methodology, Conceptualization.

Declaration of competing interest

The authors declare that they have no known competing financial interests or personal relationships that could have appeared to influence the work reported in this paper.

Appendix A

8.1 Appendix A

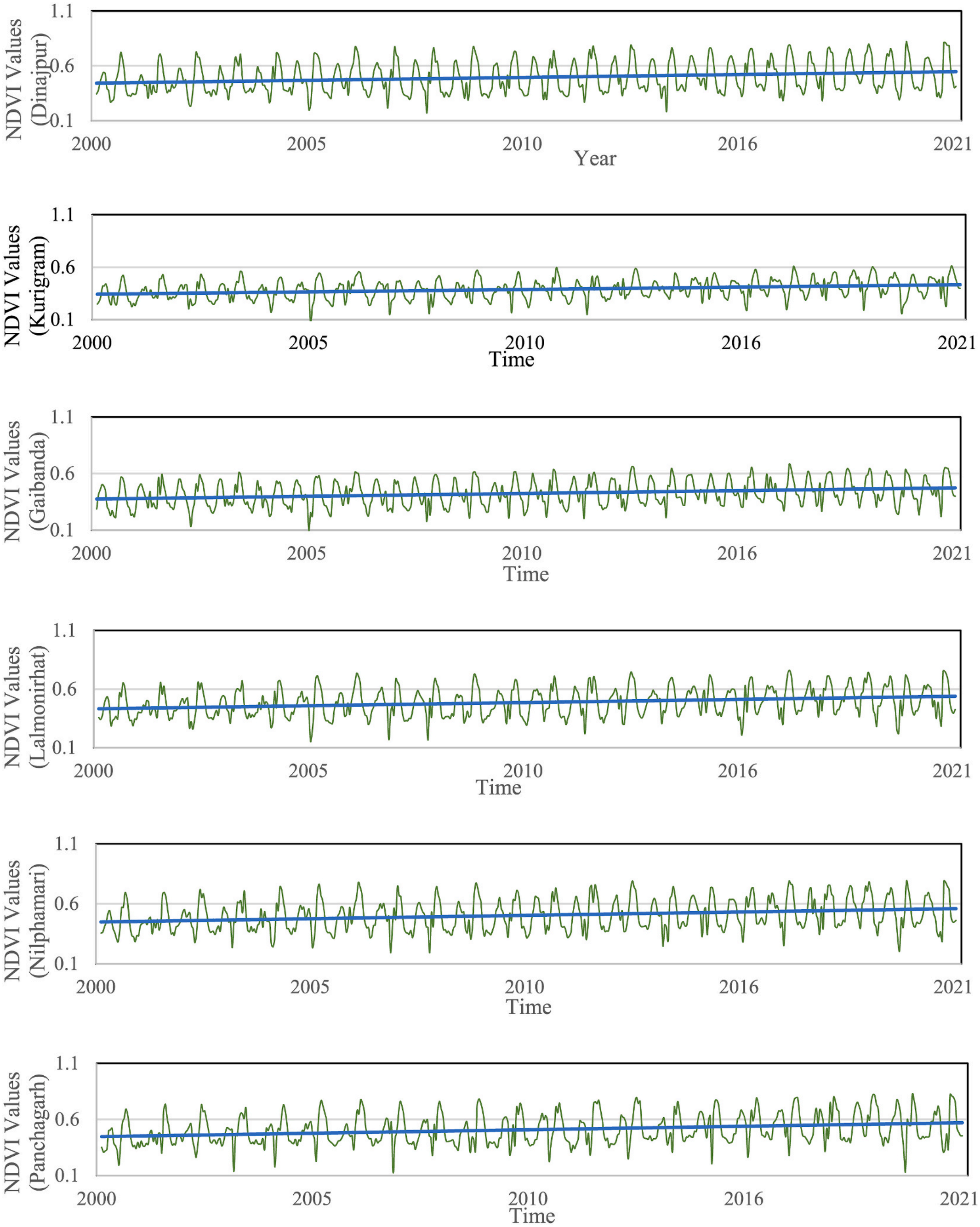

Fig. A. Times Series of NDVI values for all the districts of North-West and South-West Regions. The trends show that the values are increasing over the years.

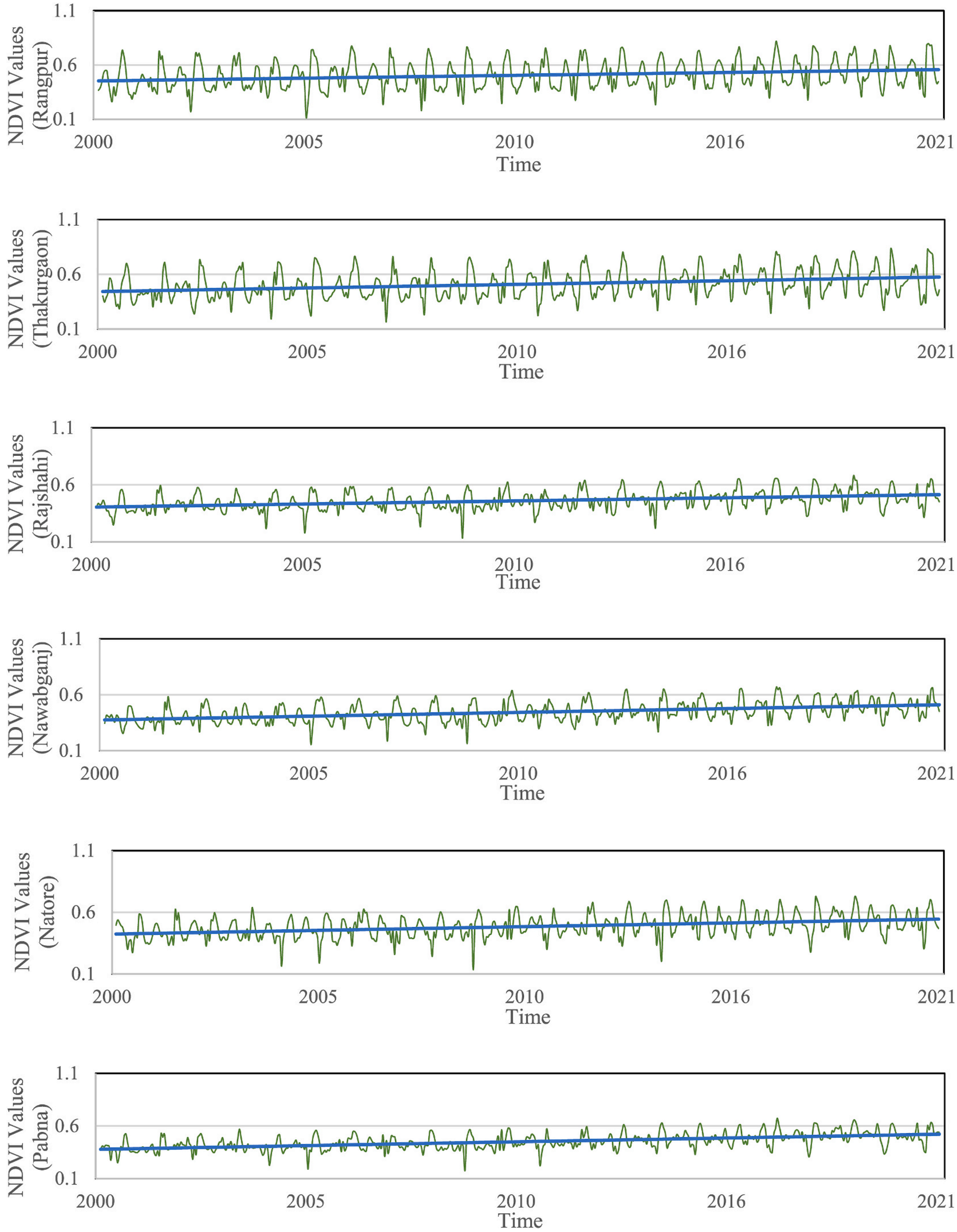

Fig. A. (*continued*).

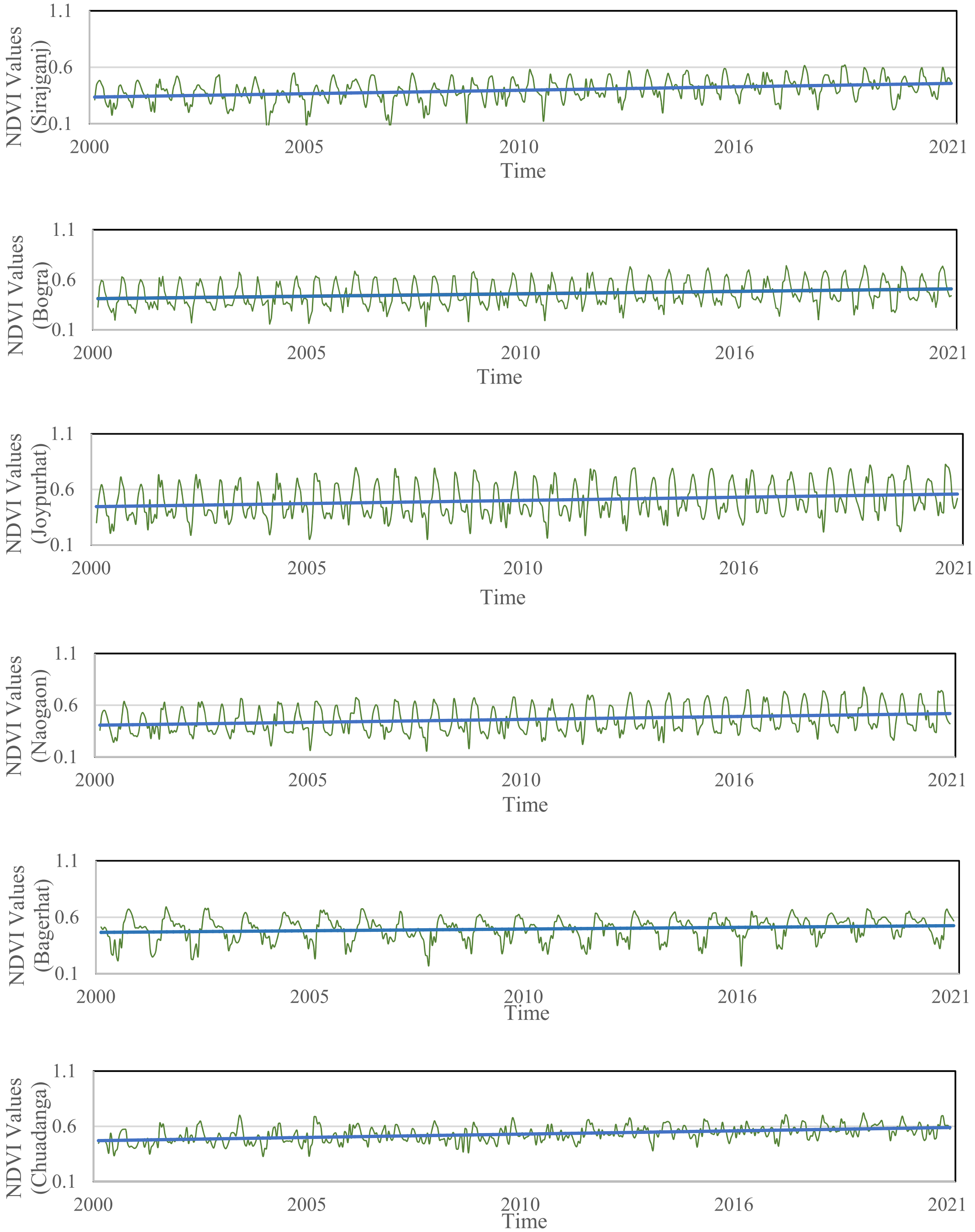

Fig. A. (*continued*).

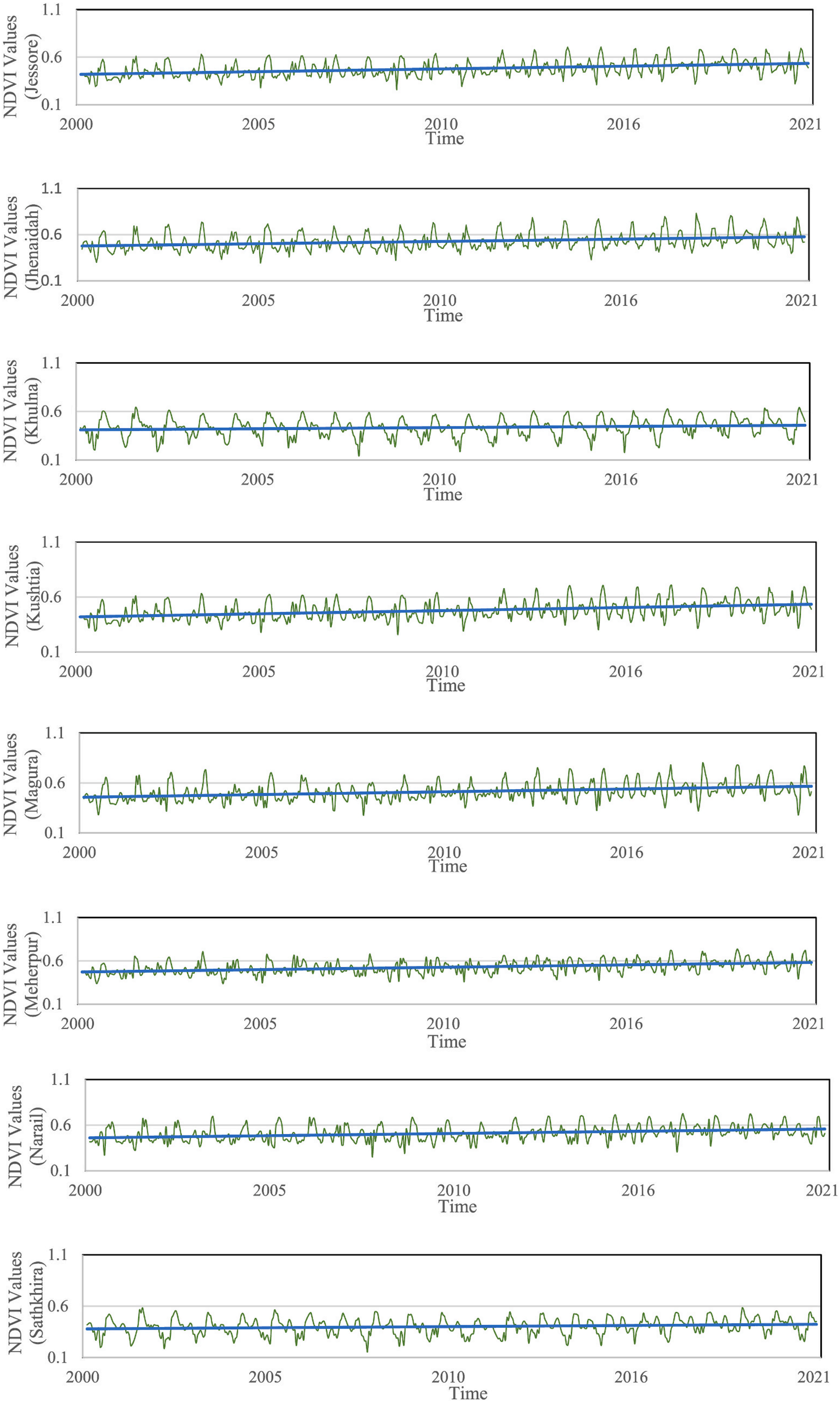

Fig. A. (*continued*).

8.2 Appendix B

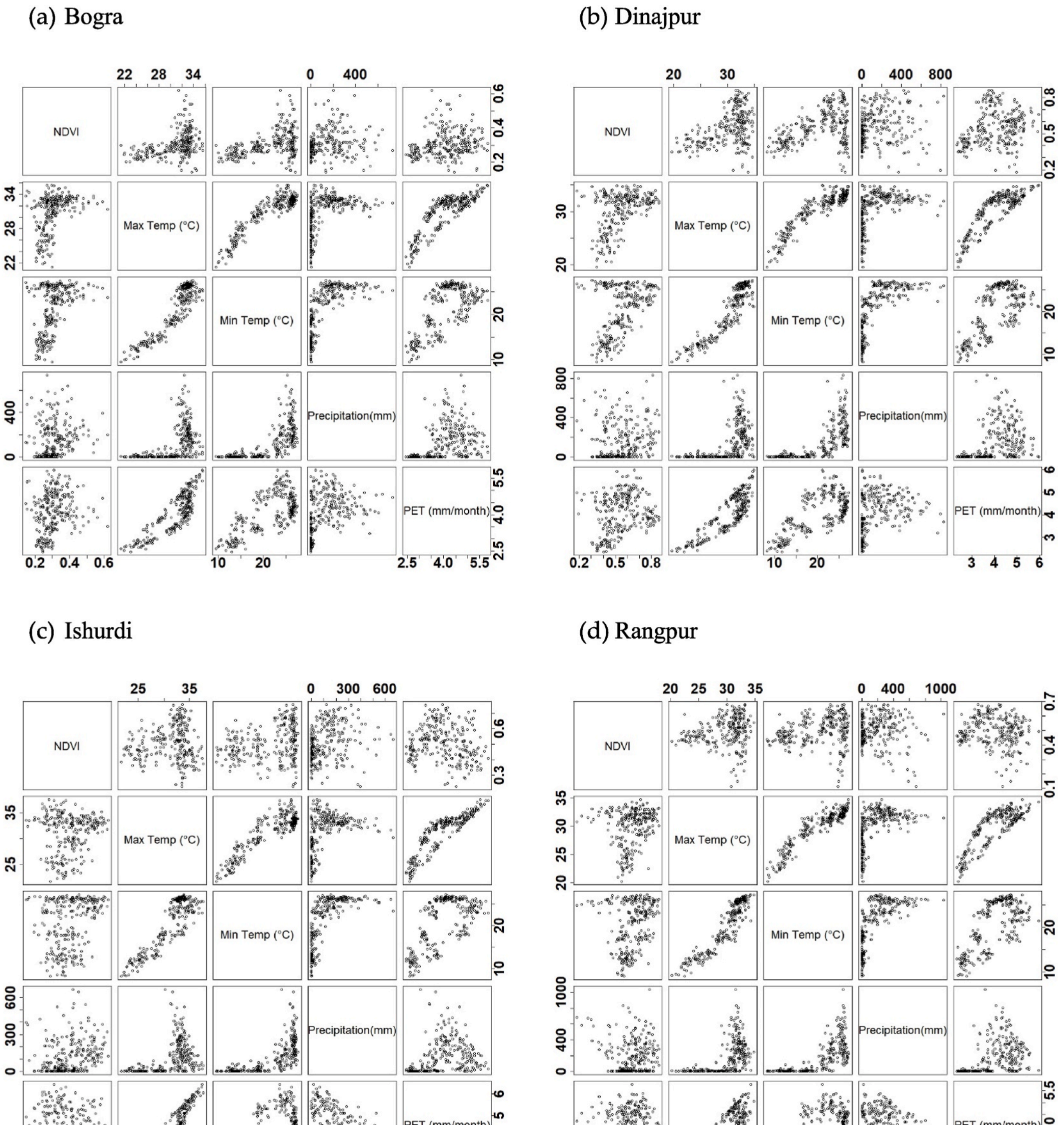

Fig. B. Multivariate Correlation Plot of (a) Bogra,(b) Dinajpur,(c) Ishurdi,(d) Rangpur,(e) Syedpur,(f) Chuadanga,(g) Jessore,(h) Khulna,(i) Mongla, and (j) Sathkhira BMD Stations

(e) Syedpur

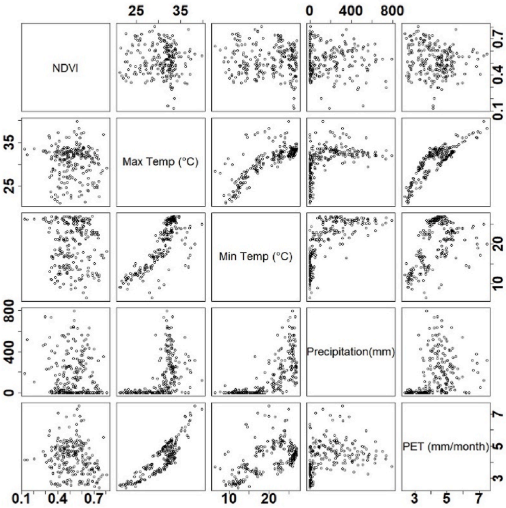

(f) Chuadanga

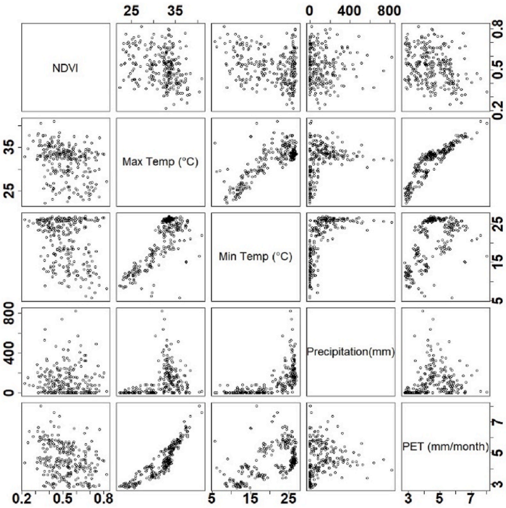

(g) Jessore

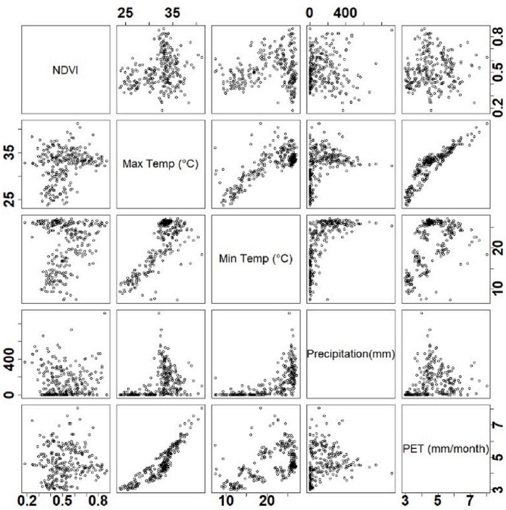

(h) Khulna

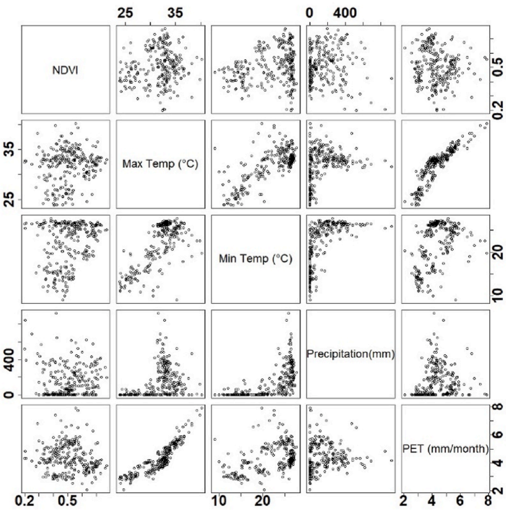

Fig. B. (*continued*).

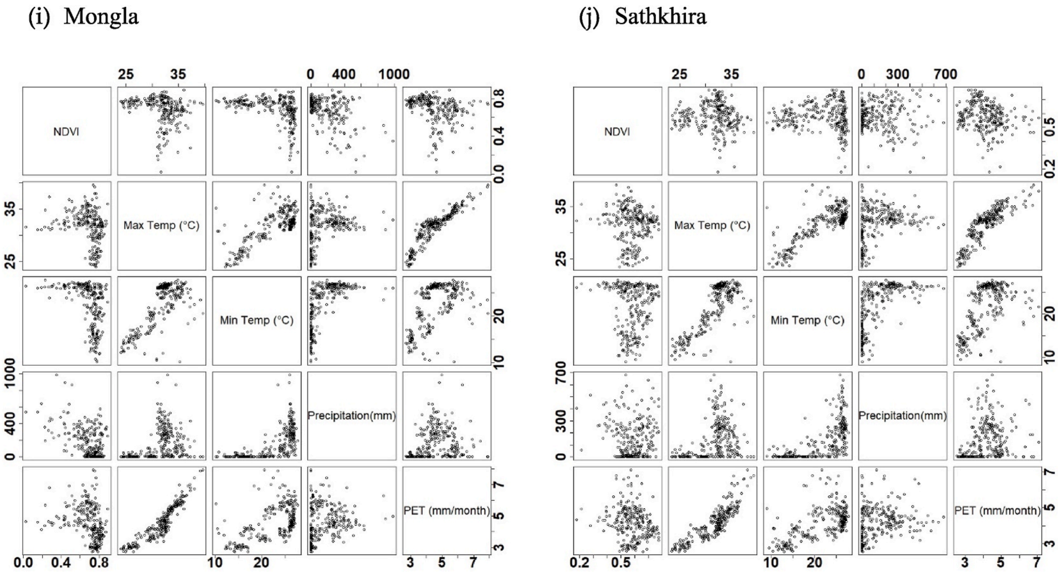

Fig. B. (*continued*).

8.3 Appendix C

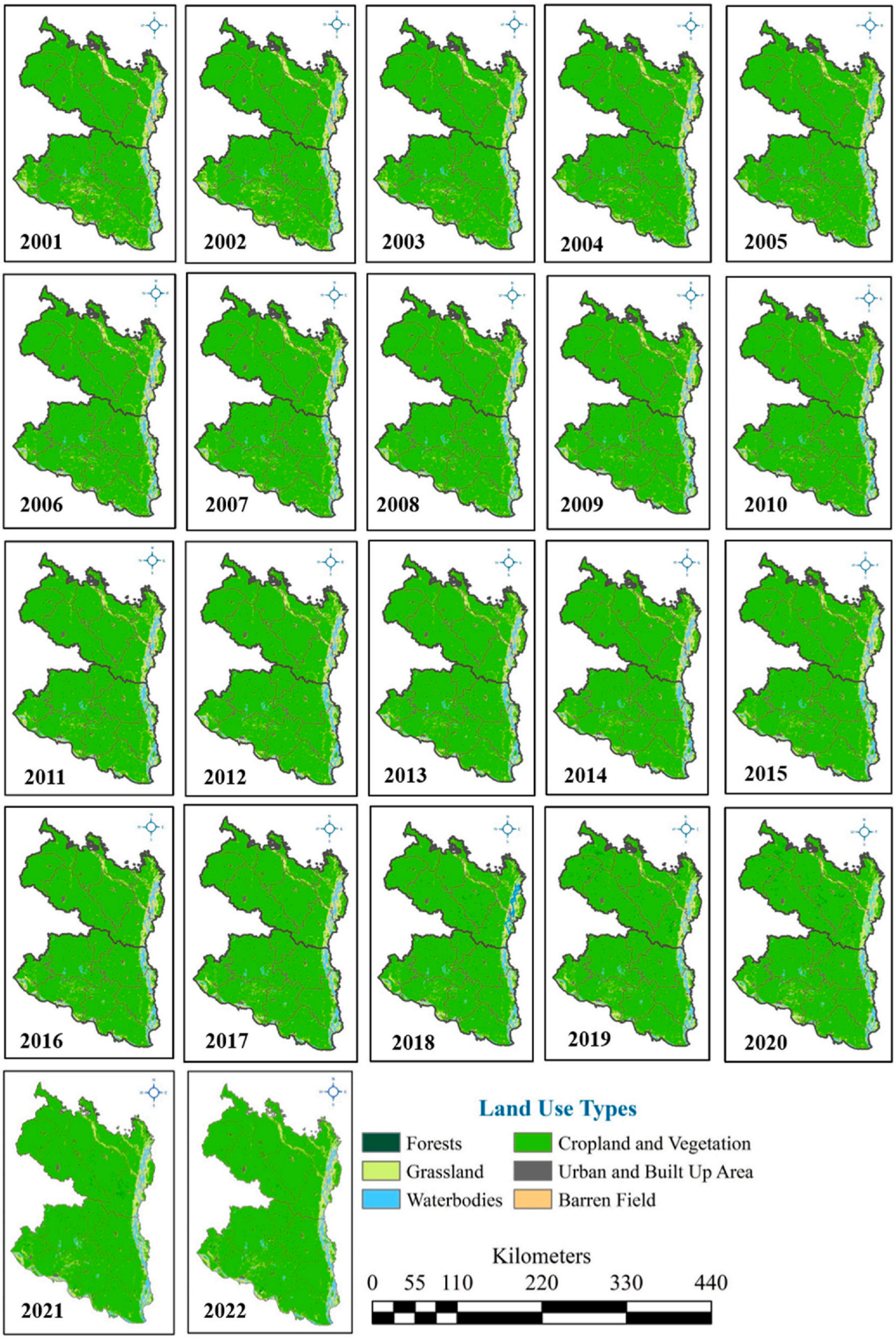

Fig. C.1. Land Cover Maps for North-West region from 2001 to 2022.

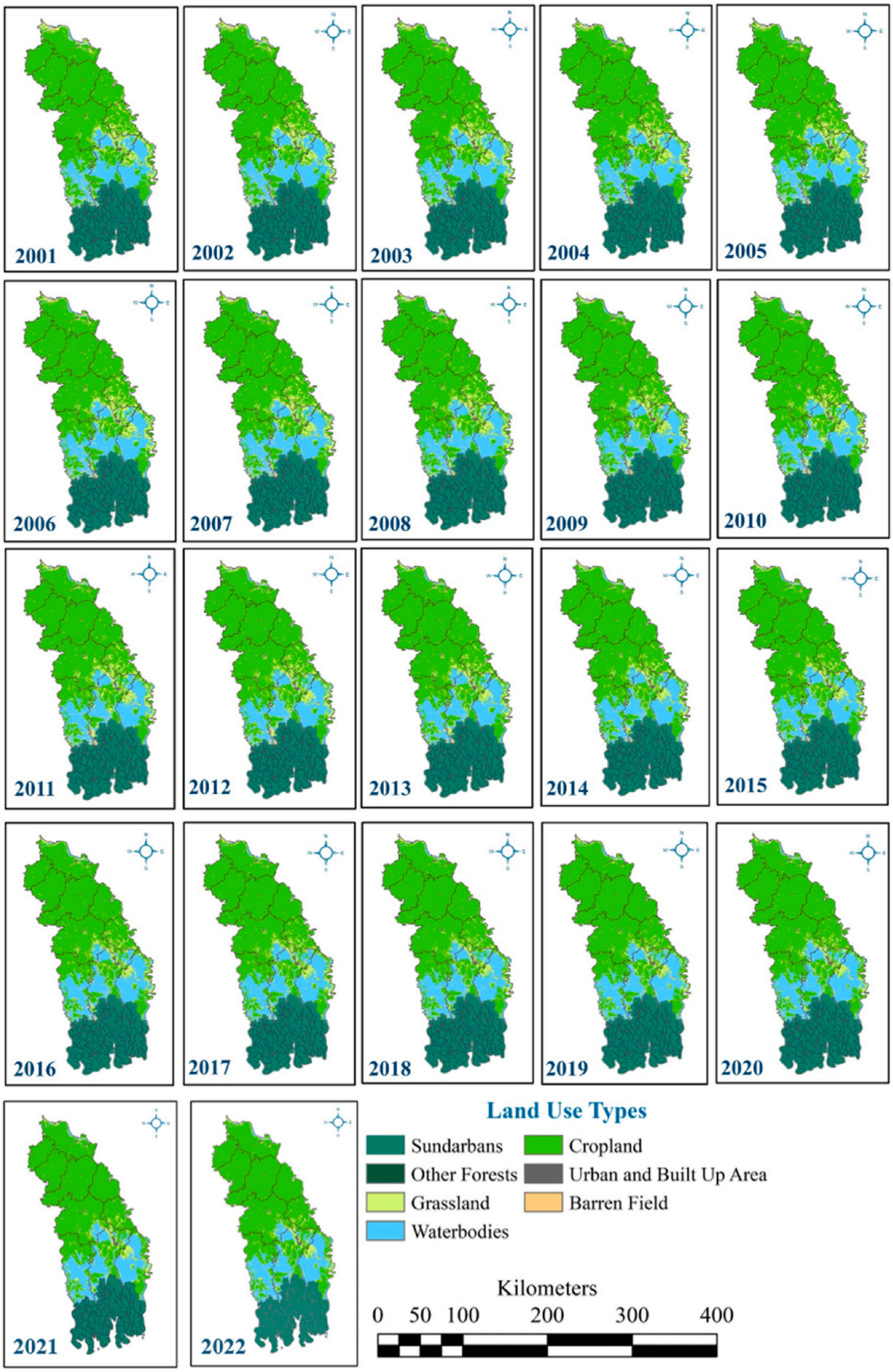

Fig. C.2. Land Cover maps for South-West region from 2001 to 2022.

8.4 Appendix D

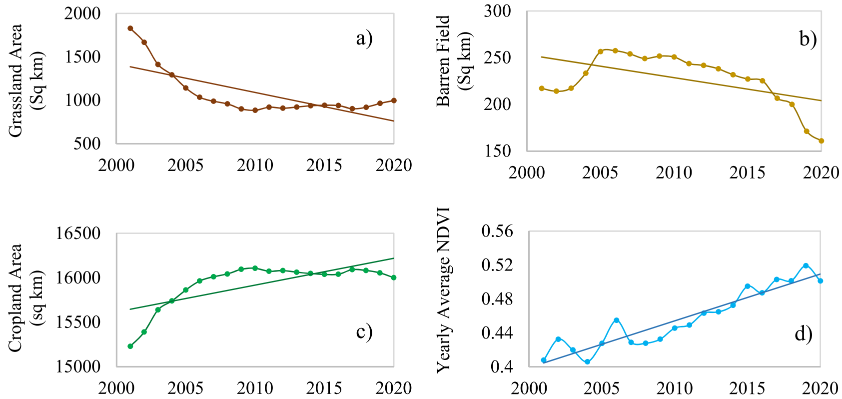

Fig. D.1. Trends of a) Grassland area decreasing, b) Barren Field decreasing, c) Cropland area increasing, d) Yearly average NDVI increasing from 2001 to 2020 for Rajshahi in North-West.

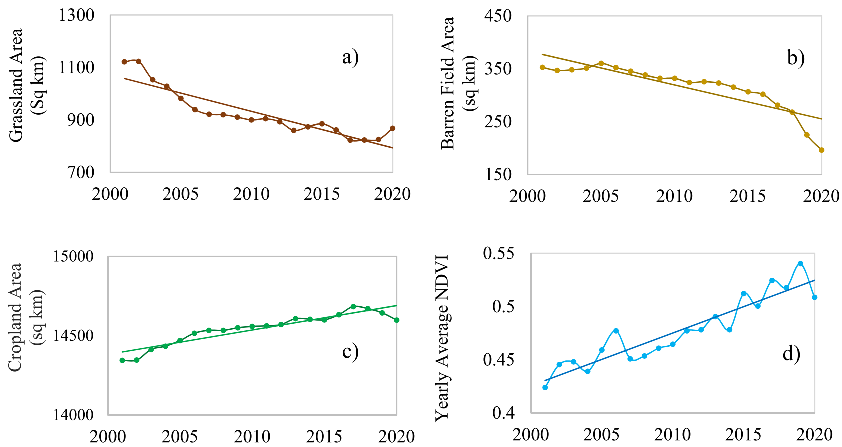

Fig. D.2. Trends of a) Grassland area decreasing, b) Barren Field decreasing, c) Cropland area increasing, d) Yearly average NDVI increasing from 2001 to 2020 for Rangpur in North-West.

References

[1] M.H. Kabir, Z. Ahmed, R. Khan, Impact of climate change on food security in Bangladesh, J. Pet. Environ. Biotechnol. 7 (2016).
[2] M.A. Mojid, M.F. Parvez, M. Mainuddin, G. Hodgson, Water table trend—a Sustainability status of groundwater development in NorthNorth-West Bangladesh *water* 11 (2019) 1182.
[3] S. Shahid, Spatial assessment of groundwater demand in Northwest Bangladesh, Int. J. Water 5 (2010) 267.
[4] N. Dey, M. Alam, A. Sajjan, M. Bhuiyan, L. Ghose, Y. Ibaraki, F. Karim, Assessing environmental and health impact of drought in the northwest Bangladesh, J. Environ. Sci. Nat. Resour. 4 (2012) 89–97.
[5] N.C. Dey, R. Saha, M. Parvez, S.K. Bala, A.S. Islam, J.K. Paul, M. Hossain, Sustainability of groundwater use for irrigation of dry-season crops in northwest Bangladesh, Groundw. Sustain. Dev. 4 (2017) 66–77.
[6] S.K. Sarkar, S.B. Ansar, K.M.M. Ekram, M.H. Khan, S. Talukdar, M.W. Naikoo, A.R.T. Islam, A. Rahman, A. Mosavi, Developing robust flood susceptibility model with small numbers of parameters in highly fertile regions of northwest Bangladesh for sustainable flood and agriculture management, Sustainability 14 (2022) 3982.
[7] M. Shamsuzzoha, Z. Islam, R.H. Khan, M.N. Amin, Status of climatic variations in North Western region of Bangladesh (1990).
[8] M. Farukh, M. Islam, L. Akter, R. Khatun, Trend and variability analysis of sunshine duration in divisional headquarters of Bangladesh, J. Environ. Sci. Nat. Resour. 12 (2021) 127–133.
[9] R Md Ferozur, C.S. Jahan, R. Arefin, Q.H. Mazumder, Groundwater potentiality study in drought prone barind tract, NW Bangladesh using remote sensing and GIS, Groundw. Sustain. Dev. 8 (2019) 205–215.
[10] M.A. Hossain, Md M. Rahman, S.S. Hasan, Application of combined drought index to assess meteorological drought in the south western region of Bangladesh, Phys. Chem. Earth Parts ABC 120 (2020) 102946.
[11] A.R. Md T. Islam, S. Shen, Z. Hu, M.A. Rahman, Drought hazard evaluation in boro paddy cultivated areas of western Bangladesh at current and future climate change conditions, Adv. Meteorol. 2017 (2017) 1–12.
[12] F. Karim, M. Mainuddin, M. Hasan, M. Kirby, Assessing the Potential Impacts of Climate Changes on Rainfall and Evapotranspiration in the Northwest Region of Bangladesh Climate 8 (2020) 94.

[13] G.K. Wedajo, M.K. Muleta, B. Gessesse, S.A. Koriche, Spatiotemporal climate and vegetation greenness changes and their nexus for Dhidhessa River Basin, Ethiopia, Environ. Syst. Res. 8 (2019) 31.
[14] F. Carreño-Conde, A.E. Sipols, C.S. de Blas, D. Mostaza-Colado, A forecast model applied to monitor crops dynamics using vegetation indices (NDVI), Appl. Sci. 11 (2021) 1859.
[15] C. Zou, H. Li, D. Chen, J. Fan, Z. Liu, X. Xu, J. Li, Z. Wang, Spatial-Temporal Changes of Carbon Source/Sink in Terrestrial Vegetation Ecosystem and Response to Meteorological Factors in Yangtze River Delta Region (China) 17 (2022).
[16] A. Essaadia, A. Abdellah, A. Ahmed, F. Abdelouahed, E. Kamal, The normalized difference vegetation index (NDVI) of the Zat valley, Marrakech: comparison and dynamics, Heliyon 8 (2022) e12204.
[17] M. Lamchin, S.W. Wang, C.-H. Lim, A. Ochir, U. Pavel, B.M. Gebru, Y. Choi, S.W. Jeon, W.-K. Lee, Understanding global spatio-temporal trends and the relationship between vegetation greenness and climate factors by land cover during 1982–2014, Glob. Ecol. Conserv. 24 (2020) e01299.
[18] Z.M. Al-Ali, M.M. Abdullah, N.B. Asadalla, M. Gholoum, A comparative study of remote sensing classification methods for monitoring and assessing desert vegetation using a UAV-based multispectral sensor, Environ. Monit. Assess. 192 (2020) 389.
[19] R. Almalki, M. Khaki, P.M. Saco, J.F. Rodriguez, Monitoring and mapping vegetation cover changes in arid and semi-arid areas using remote sensing technology: a review *remote Sens* 14 (2022) 5143.
[20] M.I. Faridatul, B. Ahmed, Assessing agricultural vulnerability to drought in a heterogeneous environment: a remote sensing-based approach, Rem. Sens. 12 (2020) 3363.
[21] J. Huang, J.L. Gómez-Dans, H. Huang, H. Ma, Q. Wu, P.E. Lewis, S. Liang, Z. Chen, J.-H. Xue, Y. Wu, F. Zhao, J. Wang, X. Xie, Assimilation of remote sensing into crop growth models: current status and perspectives, Agric. For. Meteorol. (2019). **276–277** 107609.
[22] M. Mustafa Alee, A. Danandeh Mehr, O. Akdegirmen, V. Nourani, Drought Assessment across Erbil Using Satellite Products Sustainability 15 (2023) 6687.
[23] M. Shawky, M.R. Ahmed, E. Ghaderpour, A. Gupta, G. Achari, A. Dewan, Q.K. Hassan, Remote sensing-derived land surface temperature trends over South Asia, Ecol. Inform. 74 (2023) 101969.
[24] T. Hilker, A.I. Lyapustin, F.G. Hall, R. Myneni, Y. Knyazikhin, Y. Wang, C.J. Tucker, P.J. Sellers, On the measurability of change in Amazon vegetation from MODIS, Remote Sens. Environ 166 (2015) 233–242.
[25] S. Huang, L. Tang, J.P. Hupy, Y. Wang, G. Shao, Correction to: commentary review on the use of normalized difference vegetation index (NDVI) in the era of popular remote sensing, J. For. Res. 32 (2021), 2719–2719.
[26] B.K. Kogo, L. Kumar, R. Koech, Forest cover dynamics and underlying driving forces affecting ecosystem services in western Kenya, Remote Sens. Appl. Soc. Environ. 14 (2019) 75–83.
[27] X. Lin, J. Niu, R. Berndtsson, X. Yu, L. Zhang, X. Chen, NDVI dynamics and its response to climate change and reforestation in northern China, Rem. Sens. 12 (2020) 4138.
[28] G.L. Spadoni, A. Cavalli, L. Congedo, M. Munafò, Analysis of normalized difference vegetation index (NDVI) multi-temporal series for the production of forest cartography *remote*, Sens. Appl. Soc. Environ. 20 (2020) 100419.
[29] L. Zhou, J. Wu, J. Zhang, F. Zhao, M. Liu, L. Zhao, Assessing the drought monitoring characteristic of timeseries NDVI indices in crop growing season. *2010 IEEE International Geoscience And Remote Sensing Symposium* IGARSS 2010 - 2010 IEEE International Geoscience and Remote Sensing Symposium, IEEE, Honolulu, HI, USA, 2010, pp. 2063–2066.
[30] S. Piao, H. Nan, C. Huntingford, P. Ciais, P. Friedlingstein, S. Sitch, S. Peng, A. Ahlström, J.G. Canadell, N. Cong, S. Levis, P.E. Levy, L. Liu, M.R. Lomas, J. Mao, R.B. Myneni, P. Peylin, B. Poulter, X. Shi, G. Yin, N. Viovy, T. Wang, X. Wang, S. Zaehle, N. Zeng, Z. Zeng, A. Chen, Evidence for a weakening relationship between interannual temperature variability and northern vegetation activity, Nat. Commun. 5 (2014) 5018.
[31] A. Berveglieri, N.N. Imai, L.E. Christovam, M.L.B.T. Galo, A.M.G. Tommaselli, E. Honkavaara, Analysis of trends and changes in the successional trajectories of tropical forest using the Landsat NDVI time series, Remote Sens. Appl. Soc. Environ. 24 (2021) 100622.
[32] C. Li, J. Qi, L. Yang, S. Wang, W. Yang, G. Zhu, S. Zou, F. Zhang, Regional vegetation dynamics and its response to climate change—a case study in the Tao River Basin in Northwestern China, Environ. Res. Lett. 9 (2014) 125003.
[33] Y. Liu, Y. Li, S. Li, S. Motesharrei, Spatial and temporal patterns of global NDVI trends: correlations with climate and human factors, Remote sens. 7 (2015) 13233–13250.
[34] C.L. Meneses-Tovar, NDVI as Indicator of Degradation **62**, 2012.
[35] L. Recuero, J. Litago, J.E. Pinzón, M. Huesca, M.C. Moyano, A. Palacios-Orueta, Mapping periodic patterns of global vegetation based on spectral analysis of NDVI time series, Rem. Sens. 11 (2019) 2497.
[36] M. Rhif, A. Ben Abbes, B. Martinez, I.R. Farah, An improved trend vegetation analysis for non-stationary NDVI time series based on wavelet transform, Environ. Sci. Pollut. Res. 28 (2021) 46603–46613.
[37] R.E. Kennedy, Z. Yang, W.B. Cohen, Detecting trends in forest disturbance and recovery using yearly Landsat time series: 1. LandTrendr — temporal segmentation algorithms, Remote Sens. Environ. 114 (2010) 2897–2910.
[38] H. Lyu, H. Lu, L. Mou, Learning a transferable change rule from a recurrent neural network for land cover change detection *remote sens* 8 (2016) 506.
[39] F. Rembold, M. Meroni, F. Urbano, A. Royer, C. Atzberger, G. Lemoine, H. Eerens, D. Haesen, Remote sensing time series analysis for crop monitoring with the SPIRITS software: new functionalities and use examples, Front. Environ. Sci. 3 (2015).
[40] N. Ding, D. Piao, G. Cui, S. Jeon, The impacts of climate variation and land use/cover change on net primary productivity in the Tumen River Basin, Landsc. Ecol. Eng. 18 (2022) 157–170.
[41] G. Forzieri, R. Alkama, D.G. Miralles, A. Cescatti, Satellites reveal contrasting responses of regional climate to the widespread greening of Earth, Science 356 (2017) 1180–1184.
[42] H. Machiwa, B. Tian, D. Sengupta, Q. Chen, M. Meadows, Y. Zhou, Vegetation dynamics in response to human and climatic factors in the Tanzanian Coast, Front. Earth Sci. 15 (2021) 595–605.
[43] Y. Zhu, J. Zhao, P. Lei, K. Yang, S. Zhang, X. Yin, Y. Jiang, Vegetation dynamics and their relationships with climatic factors in the "Golden Triangle" region, Environ. Sci. Pollut. Res. 29 (2022) 73029–73042.
[44] Z.K. Jabal, T.S. Khayyun, I.A. Alwan, Impact of climate change on crops productivity using MODIS-NDVI time series, Civ. Eng. J. 8 (2022) 1136–1156.
[45] S.K. Yadav, S.L. Borana, Modis derived NDVI based time series analysis of vegetation in the jodhpur area, Int. Arch. Photogram. Rem. Sens. Spatial Inf. Sci. (2019) 535–539. XLII-3/W6.
[46] N.T. Boelman, M. Stieglitz, H.M. Rueth, M. Sommerkorn, K.L. Griffin, G.R. Shaver, J.A. Gamon, Response of NDVI, biomass, and ecosystem gas exchange to long-term warming and fertilization in wet sedge tundra, Oecologia 135 (2003) 414–421.
[47] M.G. Ghebrezgabher, T. Yang, X. Yang, T. Eyassu Sereke, Assessment of NDVI variations in responses to climate change in the horn of Africa, Egypt. J. Remote sens. Space sci. 23 (2020) 249–261.
[48] J.L. May, R.D. Hollister, K.R. Betway, J.A. Harris, C.E. Tweedie, J.M. Welker, W.A. Gould, S.F. Oberbauer, NDVI changes show warming increases the length of the green season at tundra communities in northern Alaska: a fine-scale analysis, Front. Plant Sci. 11 (2020) 1174.
[49] Almouctar M.A. Sidi, Y. Wu, A. Kumar, F. Zhao, K.J. Mambu, M. Sadek, Spatiotemporal analysis of vegetation cover changes around surface water based on NDVI: a case study in Korama basin, Southern Zinder, Niger, Appl. Water Sci. 11 (2021) 4.
[50] H. Liu, L. Zheng, S. Yin, Multi-perspective analysis of vegetation cover changes and driving factors of long time series based on climate and terrain data in Hanjiang River Basin, China, Arab. J. Geosci. 11 (2018) 509.
[51] K. Mao, M. Li, C. Chen, Q. Huang, Z. Chen, F. Li, D. Chen, Estimating relationships between NDVI and climate change in Guizhou Province. Southwest China *2010 18th International Conference On Geoinformatics* 2010 18th International Conference on Geoinformatics, IEEE, Beijing, China, 2010, pp. 1–5.
[52] M. Nejadrekabi, S. Eslamian, M.J. Zareian, Spatial statistics techniques for SPEI and NDVI drought indices: a case study of Khuzestan Province, Int. J. Environ. Sci. Technol. 19 (2022) 6573–6594.
[53] J. Sun, G. Cheng, W. Li, Y. Sha, Y. Yang, On the variation of NDVI with the principal climatic elements in the Tibetan plateau, Rem. Sens. 5 (2013) 1894–1911.

[54] X. Wang, B. Jiang, J.S. Liu, Generalized R-Squared for Detecting Dependence *Biometrika*, vol. 104, 2017, pp. 129–139.
[55] H. Ahmad, Bangladesh Coastal Zone Management Status and Future Trends **22**, 2019.
[56] D. Kumar, S. Scheiter, Biome diversity in South Asia - how can we improve vegetation models to understand global change impact at regional level? Sci. Total Environ. 671 (2019) 1001–1016.
[57] S. Sruthi, M.A.M. Aslam, Agricultural drought analysis using the NDVI and land surface temperature data; a case study of raichur district *aquat. Procedia* 4 (2015) 1258–1264.
[58] W. Ullah, K. Ahmad, S. Ullah, A.A. Tahir, M.F. Javed, A. Nazir, A.M. Abbasi, M. Aziz, A. Mohamed, Analysis of the relationship among land surface temperature (LST), land use land cover (LULC), and normalized difference vegetation index (NDVI) with topographic elements in the lower Himalayan region, Heliyon 9 (2023) e13322.
[59] S.K. Yadav, S.L. Borana, Modis derived NDVI based time series analysis of vegetation in the jodhpur area, Int. Arch. Photogram. Rem. Sens. Spatial Inf. Sci. (2019) 535–539. XLII-3/W6.
[60] J.K. Basak, R.A.M. Titumir, N.C. Dey, Climate Change in Bangladesh: A Historical Analysis of Temperature and Rainfall Data 02 7 (2013).
[61] Md D.I. Bhuyan, Md M. Islam, Md E.K. Bhuiyan, A trend analysis of temperature and rainfall to predict climate change for northwestern region of Bangladesh, Am. J. Clim. Change 7 (2018) 115–134.
[62] Md R. Rahman, H. Lateh, Climate change in Bangladesh: a spatio-temporal analysis and simulation of recent temperature and rainfall data using GIS and time series analysis model, Theor. Appl. Climatol. 128 (2017) 27–41.
[63] B.M.R. Faisal, H. Rahman, N.H. Sharifee, N. Sultana, M.I. Islam, S.M.A. Habib, T. Ahammad, Integrated Application of Remote Sensing and GIS in Crop Information System—A Case Study on Aman Rice Production Forecasting Using MODIS-NDVI in Bangladesh *AgriEngineering*, vol. 2, 2020, pp. 264–279.
[64] Md A. Fattah, S.R. Morshed, Assessment of the responses of spatiotemporal vegetation changes to climatic variability in Bangladesh, Theor. Appl. Climatol. 148 (2022) 285–301.
[65] A.R.M.T. Islam, H.M.T. Islam, S. Shahid, M.K. Khatun, M.M. Ali, M.S. Rahman, S.M. Ibrahim, A.M. Almoajel, Spatiotemporal nexus between vegetation change and extreme climatic indices and their possible causes of change, J. Environ. Manag. 289 (2021) 112505.
[66] Md M. Islam, Md M.I. Mamun, Variations of NDVI and its association with rainfall and evapotranspiration over Bangladesh, Rajshahi Univ. J. Sci. Eng. 43 (2015) 21–28.
[67] D. Choudhury, K. Das, A. Das, Assessment of land use land cover changes and its impact on variations of land surface temperature in Asansol-Durgapur Development Region, Egypt. J. Remote Sens. Space Sci. 22 (2019) 203–218.
[68] N. Mahmood, M. Arshad, H. Kächele, H. Ma, A. Ullah, K. Müller, Wheat yield response to input and socioeconomic factors under changing climate: evidence from rainfed environments of Pakistan, Sci. Total Environ. 688 (2019) 1275–1285.
[69] B. Sleeter, T.R. Loveland, G.M. Domke, N. Herold, J. Wickham, N.J. Wood, Chapter 5 : land cover and land use change. Impacts, risks, and adaptation in the United States: the fourth national climate assessment, volume II, U.S. Global Change Research Program) (2018).
[70] X. Xu, S. Shrestha, H. Gilani, M.K. Gumma, B.N. Siddiqui, A.K. Jain, Dynamics and drivers of land use and land cover changes in Bangladesh, Reg. Environ. Change 20 (2020) 54.
[71] X. Xu, A.K. Jain, K.V. Calvin, Quantifying the biophysical and socioeconomic drivers of changes in forest and agricultural land in South and Southeast Asia, Global Change Biol. 25 (2019) 2137–2151.
[72] H. Dibs, A.H. Ali, N. Al-Ansari, S.A. Abed, Fusion landsat-8 thermal TIRS and OLI datasets for superior monitoring and change detection using remote sensing, Emerg. Sci. J 7 (2023) 428–444.
[73] H. Dibs, H. Sabah Jaber, N. Al-Ansari, Multi-fusion algorithms for detecting land surface pattern changes using multi-high spatial resolution images and remote sensing analysis, Emerg. Sci. J 7 (2023) 1215–1231.
[74] E. Ghaderpour, P. Mazzanti, G.S. Mugnozza, F. Bozzano, Coherency and phase delay analyses between land cover and climate across Italy via the least-squares wavelet software, Int. J. Appl. Earth Obs. Geoinformation 118 (2023) 103241.
[75] B. Zoungrana, C. Conrad, L. Amekudzi, M. Thiel, E. Da, Land use/cover response to rainfall variability: a comparing analysis between NDVI and EVI in the southwest of Burkina Faso, Climate 3 (2014) 63–77.
[76] K.R. Ahmed, S. Akter, Analysis of landcover change in southwest Bengal delta due to floods by NDVI, NDWI and K-means cluster with landsat multi-spectral surface reflectance satellite data, Remote Sens. Appl. Soc. Environ. 8 (2017) 168–181.
[77] S. Das, S.K. Sarkar, Spatio-temporal variability of vegetation and its relation to different hydroclimatic factors in Bangladesh, Heliyon 9 (2023) e18412.
[78] A.M. Dewan, Y. Yamaguchi, Md Z. Rahman, Dynamics of land use/cover changes and the analysis of landscape fragmentation in Dhaka Metropolitan, Bangladesh, Geo J. 77 (2012) 315–330.
[79] G.H. Dalposso, M.A. Uribe-Opazo, E. Mercante, R.A.C. Lamparelli, Spatial autocorrelation of ndvi and gvi indices derived from landsat/tm images for soybean crops in the western of the state of Paraná in 2004/2005 crop season, Eng. Agric. 33 (2013) 525–537.
[80] S.A. Nallan, L.J. Armstrong, A.K. Tripathy, P. Teluguntla, Hot Spot Analysis Using NDVI Data for Impact Assessment of Watershed Development *2015 International Conference On Technologies For Sustainable Development (ICTSD)* 2015 International Conference on Technologies for Sustainable Development (ICTSD), IEEE, Mumbai, India, 2015, pp. 1–5.
[81] B. Xu, B. Qi, K. Ji, Z. Liu, L. Deng, L. Jiang, Emerging hot spot analysis and the spatial–temporal trends of NDVI in the Jing River Basin of China, Environ. Earth Sci. 81 (2022) 55.
[82] L. Xu, R. Cai, H. Yu, W. Du, Z. Chen, N. Chen, Monthly NDVI prediction using spatial autocorrelation and nonlocal attention networks, IEEE J. Sel. Top. Appl. Earth Obs. Rem. Sens. 17 (2024) 3425–3437.
[83] T. Caloiero, R. Coscarelli, E. Ferrari, Application of the innovative trend analysis method for the trend analysis of rainfall anomalies in southern Italy, Water Resour. Manag. 32 (2018) 4971–4983.
[84] A. Berveglieri, N.N. Imai, L.E. Christovam, M.L.B.T. Galo, A.M.G. Tommaselli, E. Honkavaara, Analysis of trends and changes in the successional trajectories of tropical forest using the Landsat NDVI time series, Remote Sens. Appl. Soc. Environ. 24 (2021) 100622.
[85] K.H. Hamed, Trend detection in hydrologic data: the Mann–Kendall trend test under the scaling hypothesis, J. Hydrol. 349 (2008) 350–363.
[86] M. Rhif, A. Ben Abbes, B. Martinez, I.R. Farah, An improved trend vegetation analysis for non-stationary NDVI time series based on wavelet transform, Environ. Sci. Pollut. Res. 28 (2021) 46603–46613.
[87] F. Wang, W. Shao, H. Yu, G. Kan, X. He, D. Zhang, M. Ren, G. Wang, Re-Evaluation of the power of the mann-kendall test for detecting monotonic trends in hydrometeorological time series, front. Earth sci. 8 (14) (2020).
[88] R. Sinam, Rainfall trend of imphal watershed using innovative trend analysis, Appl. Ecol. Environ. Sci. 10 (2022) 368–381.
[89] Z. Şen, Trend identification simulation and application, J. Hydrol. Eng. 19 (2014) 635–642.
[90] M.S. Ashraf, M. Shahid, M. Waseem, M. Azam, K.U. Rahman, Assessment of variability in hydrological droughts using the improved innovative trend analysis method, Sustainability 15 (2023) 9065.
[91] R. Singh, S. Sah, B. Das, S. Potekar, A. Chaudhary, H. Pathak, Innovative trend analysis of spatio-temporal variations of rainfall in India during 1901–2019, Theor. Appl. Climatol. 145 (2021) 821–838.
[92] H. Wu, H. Qian, Innovative trend analysis of annual and seasonal rainfall and extreme values in Shaanxi, China, since the 1950s, Int. J. Climatol. 37 (2017) 2582–2592.
[93] Y. Chen, L. Ma, T. Liu, X. Huang, G. Sun, The synergistic effect between precipitation and temperature for the NDVI in northern China from 2000 to 2018, Appl. Sci. 13 (2023) 8425.
[94] S. Geiβ, J. Einax, Multivariate correlation analysis - a method for the analysis of multidimensional time series in environmental studies, Chemom. Intell. Lab. Syst. 32 (1996) 57–65.
[95] Y. Liu, X. Wang, M. Guo, H. Tani, N. Matsuoka, S. Matsumura, Spatial and temporal relationships among NDVI, climate factors, and land cover changes in northeast asia from 1982 to 2009, GIScience Remote Sens. 48 (2011) 371–393.

[96] M. Clavero, D. Villero, L. Brotons, Climate change or land use dynamics: do we know what climate change indicators indicate? in: S.G. Willis (Ed.), PLoS One 6 (2011) e18581.
[97] L. Deng, G. Zhu, Z. Tang, Z. Shangguan, Global patterns of the effects of land-use changes on soil carbon stocks, Glob. Ecol. Conserv. 5 (2016) 127–138.
[98] S. Yu, Z. Xu, W. Wu, D. Zuo, Effect of land use types on stream water quality under seasonal variation and topographic characteristics in the Wei River basin, China, Ecol. Indic. 60 (2016) 202–212.
[99] J. Dubé, D. Legros, Spatial Autocorrelation *Spatial Econometrics Using Microdata*, John Wiley & Sons, Inc., Hoboken, NJ, USA, 2014, pp. 59–91.
[100] D.A. Griffith, Spatial Autocorrelation *Encyclopedia Of Social Measurement* Ed K Kempf-Leonard, Elsevier, New York, 2005, pp. 581–590.
[101] R.P. Haining, in: N.J. Smelser, P.B. Baltes (Eds.), Spatial Autocorrelation *International Encyclopedia Of the Social & Behavioral Sciences*, Pergamon, Oxford, 2001, pp. 14763–14768.
[102] P.A.P. Moran, Notes on continuous stochastic phenomena, Biometrika 37 (1950) 17–23.
[103] J.K. Ord, A. Getis, Local spatial autocorrelation statistics: distributional issues and an application, Geogr. Anal. 27 (2010) 286–306.
[104] P. Songchitruksa, X. Zeng, Getis–ord spatial statistics to identify hot spots by using incident management data, Transp. Res. Rec. J. Transp. Res. Board 2165 (2010) 42–51.
[105] H.B. Mann, Nonparametric Tests against Trend, Econometrica vol. 13 (1945) 245.
[106] P.K. Sen, Estimates of the regression coefficient based on kendall's Tau, J. Am. Stat. Assoc. 63 (1968) 1379–1389.
[107] S. Yue, C. Wang, The mann-kendall test modified by effective sample size to detect trend in serially correlated hydrological series, Water Resour. Manag. 18 (2004) 201–218.
[108] Z. Şen, Innovative Trend Analysis Methodology, 2012.
[109] G.H. Hargreaves, R.G. Allen, History and evaluation of Hargreaves evapotranspiration equation, J. Irrig. Drain. Eng. 129 (2003) 53–63.
[110] Y. Aydın, Assessing of evapotranspiration models using limited climatic data in Southeast Anatolian Project Region of Turkey, PeerJ 9 (2021) e11571.
[111] R.D.S. Nóia Júnior, C.W. Fraisse, V.A. Cerbaro, M.A.Z. Karrei, N. Guindin, Evaluation of the hargreaves-samani method for estimating reference evapotranspiration with ground and gridded weather data sources, Appl. Eng. Agric. 35 (2019) 823–835.
[112] M. Todorovic, B. Karic, L.S. Pereira, Reference evapotranspiration estimate with limited weather data across a range of Mediterranean climates, J. Hydrol. 481 (2013) 166–176.
[113] T. Chai, R.R. Draxler, Root mean square error (RMSE) or mean absolute error (MAE)? – Arguments against avoiding RMSE in the literature, Geosci. Model Dev. 7 (2014) 1247–1250.
[114] C. Willmott, K. Matsuura, Advantages of the mean absolute error (MAE) over the root mean square error (RMSE) in assessing average model performance, Clim. Res. 30 (2005) 79–82.
[115] D. Althoff, L.N. Rodrigues, Goodness-of-fit criteria for hydrological models: model calibration and performance assessment, J. Hydrol. 600 (2021) 126674.
[116] M.E. Awuh, P.O. Japhets, M.C. Officha, A.O. Okolie, I.C. Enete, A correlation analysis of the relationship between land use and land cover/land surface temperature in abuja municipal, FCT, Nigeria, J. Geogr. Inf. Syst. 11 (2019) 44–55.
[117] A.-A. Kafy, N.N. Dey, A. Al Rakib, Z.A. Rahaman, N.M.R. Nasher, A. Bhatt, Modeling the relationship between land use/land cover and land surface temperature in Dhaka, Bangladesh using CA-ANN algorithm, Environ. Chall. 4 (2021) 100190.